Molecular Pharmacology Fast Forward. Published on December 5, 2014 as DOI: 10.1124/mol.114.093211
This article has not been copyedited and formatted. The final version may differ from this version.

A Peptide Mimicking a Region in Proliferating Cell Nuclear Antigen (PCNA) Specific to Key Protein Interactions is Cytotoxic to Breast Cancer

Shanna J. Smith, Long Gu, Elizabeth A. Phipps, Lacey E. Dobrolecki, Karla S. Mabrey, Pattie Gulley, Kelsey L. Dillehay, Zhongyun Dong, Gregg B. Fields, Yun-Ru Chen, David Ann, Robert J. Hickey, and Linda H. Malkas

Author Affiliations

Department of Molecular and Cellular Biology (S.J.S., L.G., L.H.M.), Department of Molecular Medicine (R.J.H.), and Department of Diabetes and Metabolic Diseases Research (Y.-R.C. and D.A.), Beckman Research Institute at City of Hope, Duarte, California; Department of Medical and Molecular Genetics (E.A.P.) and Department of Medicine (K.S.M., P.G.), Indiana University School of Medicine, Indianapolis, Indiana; Lester and Sue Smith Breast Center, Baylor College of Medicine, Houston, Texas (L.E.D.); Department of Internal Medicine, University of Cincinnati College of Medicine, Cincinnati, Ohio (K.L.D., Z.D.); Torrey Pines Institute for Molecular Studies, Port St. Lucie, Florida (G.B.F.)

Molecular Pharmacology Fast Forward. Published on December 5, 2014 as DOI: 10.1124/mol.114.093211
This article has not been copyedited and formatted. The final version may differ from this version.

Running Title: A Peptide Mimicking PCNA is Cytotoxic in Breast Cancer

Corresponding Author (for submission and review process):

Shanna J. Smith, Beckman Research Institute, City of Hope, 1500 E. Duarte Rd., Duarte, CA 91010. *Email:* shsmith@coh.org

Corresponding Author (after publication):

Linda H. Malkas, Beckman Research Institute, City of Hope, 1500 E. Duarte Rd., Duarte, CA 91010. *Email:* lmalkas@coh.org

Text: 22 pages

Figures: 9, 3 supplemental

References: 60

Abstract: 242 words

Introduction: 749 words

Discussion: 1327 words

ABBREVIATIONS: BRCA1: breast cancer susceptibility gene 1; CAF-1: chromatin assembly factor-1; 5-FAM: 5-carboxyfluorescein; FEN-1: flap structure-specific endonuclease 1; IDCL: interdomain connector loop; MTT: 3-(4,5-Dimethylthiazol-2-yl)-2,5-diphenyltetrazolium bromide; PBMC: peripheral blood mononuclear cells; PCNA: proliferating cell nuclear antigen; caPCNA: cancer-associated proliferating cell nuclear antigen; nmPCNA: nonmalignant proliferating cell nuclear antigen; pI: isoelectric point; PIP-box: PCNA-interacting protein box; TLS: translesion synthesis.

Molecular Pharmacology Fast Forward. Published on December 5, 2014 as DOI: 10.1124/mol.114.093211
This article has not been copyedited and formatted. The final version may differ from this version.

ABSTRACT

Proliferating cell nuclear antigen (PCNA) is a highly conserved protein necessary for proper component loading during the DNA replication and repair process. Proteins make a connection within the interdomain connector loop (IDCL) of PCNA, and much of the regulation is a result of the inherent competition for this docking site. If this target region of PCNA is modified, the DNA replication and repair process in cancer cells is potentially altered. Exploitation of this cancer-associated region has implications in targeted breast cancer therapy. In the present communication, we characterize a novel peptide (caPeptide) that has been synthesized to mimick the sequence identified as critical to the cancer-associated isoform of PCNA (caPCNA). This peptide is delivered into cells using a nine-arginine linking mechanism, and the resulting peptide (R9-cc-caPeptide) exhibits cytotoxicity in a triple negative breast cancer cell line, MDA-MB-436, while having less of an effect on the normal counterparts (MCF10A and primary breast epithelial cells). The novel peptide was then evaluated for cytotoxicity using various *in vivo* techniques, including: ATP activity assays, flow cytometry, and clonogenetic assays. This cytotoxicity has been observed in other breast cancer cell lines (MCF 7 and HCC 1937), and other forms of cancer (pancreatic and lymphoma). R9-cc-caPeptide has also been shown to block the association of PCNA with chromatin. Alanine scanning of the peptide sequence, combined with preliminary *in silico* modeling, gives insight to the disruptive ability and the molecular mechanism of action of the therapeutic peptide *in vivo*.

Molecular Pharmacology Fast Forward. Published on December 5, 2014 as DOI: 10.1124/mol.114.093211
This article has not been copyedited and formatted. The final version may differ from this version.

Introduction

Proliferating cell nuclear antigen (PCNA) is an evolutionarily conserved protein that is critically important to many cellular processes (Prosperi, 1997). During DNA replication, this 36 kDa protein forms a homotrimer encircling the DNA strand and acts as a scaffold to systematically load proteins and enzymes. Immunohistochemical (IHC) staining of breast cancer tissues samples exhibits a pattern of increased PCNA expression (Tahan et al., 1993), as compared to unaffected epithelial tissue adjacent to the tumor site. This increased PCNA expression in breast cancer is associated with axillary node status, p53 overexpression, shorter disease-free survival, and shorter overall survival (Chu et al., 1998).

Mutagenic analyses show the DNA replication machinery derived from malignant breast cell lines and actual tumor tissue replicate DNA in a significantly more error-prone manner, as compared to the replication machinery derived from nonmalignant counterparts (Sekowski et al., 1998). A structural comparison of the components from both normal and malignant cell lines using two-dimensional SDS- PAGE analysis revealed a unique form of PCNA present only in malignant breast cells (Bechtel et al., 1998). These malignant cells harbor an additional isoform of PCNA with an acidic isoelectric point (pI), as opposed to the normal cell only containing PCNA with a basic pI. Similar PCNA profiles are present in other types of cancer, including neuroblastoma (Sandoval et al., 2005), hepatic carcinoma (Venturi et al., 2008), high-grade prostatic intraepithelial neoplasia and prostate cancer (Wang et al., 2011). The newly identified cancer-associated acidic isoform of PCNA (caPCNA) results from a set of post-translational modifications (Hoelz et al., 2006). Previous studies have shown that PCNA can be post-translationally modified by phosphorylation (Wang et al., 2006), acetylation (Naryzhny and Lee, 2004), ubiquitination, and sumolytion (Garg and Burgers, 2005; Hoege et al., 2002; Kannouche

Molecular Pharmacology Fast Forward. Published on December 5, 2014 as DOI: 10.1124/mol.114.093211
This article has not been copyedited and formatted. The final version may differ from this version.

and Lehmann, 2004; Kannouche et al., 2004; Kemp et al., 2009; Krijger et al., 2011; Sabbioneda et al., 2008; Stelter and Ulrich, 2003; Watanabe et al., 2004). These modifications act as regulators of PCNA activity in normal cellular processes, while others have yet to be fully understood. These uncharacterized alterations could be key to cancer development and progression.

A PCNA monomer has two topologically similar domains linked head to tail. These domains are connected by a crossover loop, referred to as the "interdomain connector loop" (IDCL). X-ray crystallograms of PCNA have shown that PCNA exhibits increased mobility within the IDCL (Bruning and Shamoo, 2004), indicating that a number of conformations are possible in this region to accommodate a myriad of interactions. In fact, a majority of the proteins interacting with PCNA do so within the IDCL via a conserved motif known as the "PCNA-interacting protein" (PIP)-box. The PIP-box generally consists of an extended N-terminal region, a central conserved region containing hydrophobic residues, a 3_{10} helix, and a C-terminal region that varies in length. The single-turn 3_{10} helix displays a side chain residue that fits like a "plug" in the hydrophobic pocket of the PCNA IDCL (Bruning and Shamoo, 2004). The helical conformation brings the LXXFF region to the side of the structure, allowing for hydrogen bonding with the glutamine within the IDCL (Chapados et al., 2004).

The commonality of PCNA-binding motifs suggests that regulation depends on the competition of proteins within the interaction site, making the IDCL of PCNA a fascinating therapeutic target (Kontopidis et al., 2005). Much of the recent work to inhibit PCNA interactions focuses on blocking the IDCL region by synthesizing peptides and small molecules to mimic the binding of partner proteins, such as p21 (Kontopidis et al., 2005; Punchihewa et al., 2012; Warbrick, 2006; Zheleva et al., 2000). These p21-derived agents can specifically disrupt

Molecular Pharmacology Fast Forward. Published on December 5, 2014 as DOI: 10.1124/mol.114.093211
This article has not been copyedited and formatted. The final version may differ from this version.

protein-PCNA interactions, and have been shown to block replication and cell cycle progression, both *in vitro* and *in vivo*. This approach, however, most likely will not have the specificity required to only block PCNA-protein interactions in cells that harbor the caPCNA isoform, such as cancer cells.

We have successfully developed a rabbit polyclonal antibody that specifically recognizes the cancer-associated isoform of PCNA (caPCNAab). We then synthesized a peptide mimicking this region identified as specific to caPCNA, which is within the IDCL of PCNA and critical to protein binding. In the present communication, we show the peptide exhibits cytotoxicity in a triple-negative breast cancer cell line (MDA-MB-436). The peptide inhibits binding of PCNA-interacting proteins required for DNA replication and repair, preventing normal cellular function, and eventually resulting in cellular death. Because of the peptide's specificity to caPCNA, it has the therapeutic capability to target DNA replication and repair in cells harboring the caPCNA isoform.

Materials and Methods

Antibody production. caPCNA antibodies were produced by Zymed Laboratories (South San Francisco, CA) and Yenzym Antibodies (South San Francisco, CA). All animal work was approved by the Institutional Animal Care and Use Committee (IUCAC). Peptides of varying sequence lengths within the PCNA IDCL were synthesized. To increase the length of the peptide and improve antigenicity, a spacer arm consisting of CGGG was added to the N-terminus of each antigenic peptide. The peptide was covalently conjugated to keyhole limpit hemocyanin (KLH) and 100 μg was injected into female rabbits (two per peptide) in complete Freund's adjuvant. Four weeks after the initial injection, the rabbits were boosted with a second injection. The boost was repeated after another four weeks and, 12 days after the

Molecular Pharmacology Fast Forward. Published on December 5, 2014 as DOI: 10.1124/mol.114.093211
This article has not been copyedited and formatted. The final version may differ from this version.

final boost, the rabbits were bled and 20 mL of serum was obtained. Affinity purification of the antisera was performed using the antigens' peptide-coupled chromatography matrix. The affinity matrix was transferred to the antisera, diluted 1:1 with PBS and mixed thoroughly at 4°C for 2 hours. After collecting the flow through, the gel was washed extensively and the antibody was eluted with a low pH elution buffer (0.1 M glycine, pH 2.5). The pH was neutralized with Tris buffer and the eluted solution was dialyzed against PBS. A 0.1% sodium azide solution was added to the final purified antibody.

Peptide production. All peptides (excluding the all-D peptide) were synthesized and isolated to greater than 95% purity by AnaSpec (San Jose, CA). The all-D peptide was synthesized on a Protein Biotechnologies PS3 Synthesizer, purified by reversed-phase HPLC, and characterized by MALDI-TOF mass spectrometry. The peptides were received in powder form and stored at -20°C. Prior to use, each peptide was solubilized in PBS (Mediatech, Manassas, VA) to a concentration of 10 mM, and aliquots were stored at -20°C.

Cell culture. All cancer cell lines were cultured according to procedures established by the American Type Culture Collection (ATCC). MCF7 cells were cultured in Dulbecco's Modified Eagle Medium (DMEM) (Mediatech, Manassas, VA) supplemented with 10% fetal bovine serum and 1% penicillin/streptomycin. PaCa-2 cells were cultured in DMEM supplemented with 10% fetal bovine serum, 2.5% horse serum, and 1% penicillin/streptomycin. MDA-MB-436 cells were cultured in MEM (Gibco Life Technologies, Grand Island, NY) supplemented with 10% fetal bovine serum, 1% penicillin/streptomycin, 2% MEM essential vitamins, 1% sodium pyruvate, and 1 mM HEPES. MCF10A cells were cultured in DMEM/F-12 (50:50) (Mediatech, Manassas, VA) supplemented with 5% donor horse serum, 20 ng/ml epidermal growth factor (EGF), 10 μg/ml insulin, 100 μg/ml hydrocortisone, and 100 ng/ml cholera toxin. Human mammary epithelial cells (HMEC) were obtained from Invitrogen Life Technologies (Grand Island, NY) and cultured according to manufacturer's specifications in the provided HuMEC Ready Medium. U937 and HCC1937 cells were cultured in RPMI-1640 medium (Mediatech, Manassas, VA) supplemented with 10% fetal bovine serum. HCC1937 BRCA+ cells were obtained from

Molecular Pharmacology Fast Forward. Published on December 5, 2014 as DOI: 10.1124/mol.114.093211
This article has not been copyedited and formatted. The final version may differ from this version.

Dr. Stephen Elledge (Harvard Medical School), and selectively cultured with an addition of 1 μg/ml puromycin. All cell cultures were maintained at 37°C supplemented with 5% CO_2.

Cellular fractionation. Cultured MCF7 cells were homogenized with a homogenization buffer (200 mM sucrose, 50 mM HEPES-KOH pH 7.5, 5 mM KCl, 5 mM $MgCl_2$, 2 mM DTT, and 1 mM PMSF) and pelleted. The resulting supernatant was supplemented with 5 mM EDTA and 5 mM EGTA to inhibit protein degradation. Differential centrifugation was used to pellet the mitochondria and microsomes and the resulting supernatant was collected and stored at -80°C until used.

Two-Dimensional Polyacrylamide Gel Electrophoresis (2D-PAGE). MCF7 fractions (150 μg) were desalted using Protein Desalting Spin Columns (Pierce, Rockford, IL) and lyophilized in a speed vac (ATR, Laurel, MD). The lyophilized samples were rehydrated in equal parts diH_20 and first dimension sample buffer (9 M Urea, 2% Triton X-100, 5% β-mercaptoethanol, 1.6% Bio-lyte 5/7 ampholyte, and 0.4% Bio-lyte 3/10 ampholyte), loaded in a first-dimension tube gel (9.2 M urea, 4% acrylamide, 1.6% pH 5-7 ampholytes, 0.4% pH 3-10 ampholytes, and 2% Triton X-100), then overlaid with 30μl of first dimension sample overlay buffer (9 M Urea, 0.8% Bio-lyte 5/7 ampholyte, 0.2% Bio-lyte 3/10 ampholyte, and 0.0025% bromophenol blue). Isoelectric focusing of the polypeptides was achieved using 10 mM NaOH and 10 mM H_3PO_4 to create a pH gradient. Focused tube gels were transferred to a 12% polyacrylamide-SDS gel to resolve the second dimension by molecular weight.

Western Blot Analysis. The resolved proteins were electrophoretically transferred from the slab gel to polyvinylidene difluoride (PVDF) membranes. Membranes were blocked for 30 minutes in buffer containing 10 mM Tris-HCl, pH 7.5, 100 mM NaCl, 2.5 mM EDTA pH 8.0, 0.1% Tween 20, and 5% non-fat dry milk, then exposed to either PCNA PC10 (1:2000 dilution) (Santa Cruz Biotechnology, Santa Cruz, CA) or the epitope-mapping anti-rabbit caPCNA antibodies (1:500 dilution) for 90 minutes. Blots were washed with TNE (10 mM Tris-HCl, pH 7.5, 100 mM NaCl, and 2.5 mM EDTA pH 8.0) to remove background. Membranes were then incubated with horseradish peroxidase secondary antibodies for one

Molecular Pharmacology Fast Forward. Published on December 5, 2014 as DOI: 10.1124/mol.114.093211
This article has not been copyedited and formatted. The final version may differ from this version.

hour. Final TNE washes were performed and immunodetection was performed using the Visualizer Spray & Glow chemiluminescent system (Millipore, Billerica, MA).

Immunohistochemical (IHC) Staining. Formalin-fixed, paraffin-embedded sections of breast tissue (normal and DCIS cases) were stained with the panel of purified caPCNA antibodies and the commercially available PC 10 (Santa Cruz Biotechnology, Santa Cruz, CA) using the OptiView DAB IHC Detection Kit (Ventana Medical Systems, Tucson, AZ). All antibody staining was conducted and antibody dilutions were optimized (1:2500 to 1:7500) on the Ventana BenchMark XT IHC/ISH staining module (Ventana Medical Systems, Tucson, AZ) to eliminate variability.

***In vitro* cytotoxicity of R9-cc-caPeptide.** Exponentially growing ($3x10^3$ cells/well) MDA-MB-436 cells were seeded in 96-well plates. In octuplicate, increasing concentrations of peptide was added to each well and incubated for 48 hours at 37°C with 5% CO_2. Cell viability was determined using the CellTiter-Glo Luminescent Cell Viability Assay (Promega, Madison, WI), according to manufacturer's instructions. Activity was calculated as the % of cells killed/concentration versus control cells with no R9-cc-caPeptide treatment, where 0% indicates no cell death (high ATP levels) and 100% indicates complete cell death (low or no ATP levels). Data were analyzed and EC_{50} values were determined following the guidelines described in Sebaugh (Gilmore et al., 2003), and using the sigmoidal dose-response equation in GraphPad Prism 5 software (La Jolla, CA).

MTT Cell Viability Assay. MDA-MB-436 cells ($5x10^3$ cells/well) were seeded in 96-well plates and incubated overnight at 37°C with 5% CO_2. In octuplicate, cells were then treated for 24 hours with increasing concentrations of caPeptide and its variants. After 24 hours, the medium was removed; cells were then washed with PBS and incubated with MTT solution (500 μg/mL thiazolyl blue tetrazolium bromide) for 4 hours. The MTT solution was then removed, and cells were resuspended in dimethyl sulfoxide (DMSO). The absorbance at λ = 570 nm was then measured for each well. Cell proliferation

Molecular Pharmacology Fast Forward. Published on December 5, 2014 as DOI: 10.1124/mol.114.093211
This article has not been copyedited and formatted. The final version may differ from this version.

was calculated as the % of surviving cells/concentration versus control cells with no R9-cc-caPeptide treatment.

Apoptotic Evaluation of Cells. Exponentially growing cells ($1x10^6$ cells/well) were seeded in a 12-well plate. In triplicate, the appropriate concentration of peptide was then added to each well. Cells were treated for 48 hours, collected, washed twice with ice cold PBS (Mediatech, Manassas, VA), and resuspended in PBS with 1 μg/ml propidium iodide (PI). The cellular PI intensity was measured using the CyAn ADP 9 Color (Beckman Coulter, Indianapolis, IN) flow cytometer. Gates were set using untreated MDA-MB-436 cells (control), with 50,000 events counted per sample. % cell death for each sample was calculated relative to control.

For Annexin V staining, cells were treated with 50 or 100 μM of either R9-cc-caPeptide or R9-cc-scrambled for 4, 8 and 24h. After trypsinization, cells were washed twice with cold PBS and collected by centrifugation at 1000 rpm. Cells were then resuspended in 1X Binding Buffer at a concentration of 1 x 10^6 cells/ml and 100 μl of the suspension (1 x 10^5 cells) was transferred to a polystyrene round-bottom tube. Cells were subsequently stained with FITC-conjugated Annexin V (4 μl) and propidium iodide (PI) (50 μg/ml, 5 μl). The mixture was gently vortexed and incubated for 15 minutes at room temperature and 1 x Binding Buffer (400 μl) was added to each tube prior to analysis using flow cytometry.

Colony Formation Assay. MDA-MB-436 cells were seeded in 25 cm^3 flasks ($3x10^5$ cells/flask) and incubated overnight at 37°C with 5% CO_2. Each flask was then treated for one (1) hour with increasing concentrations of R9-cc-caPeptide and R9-cc-scrambled peptide. After one hour, the medium was removed from the treated flasks and replaced by 1 mL of 0.25% trypsin (Invitrogen, Grand Island, NY) to resuspend cells. Each treatment set of cells were then plated into 10 cm dishes at a density of 750 cells/dish, with 3 dishes for each concentration. Dishes were incubated for 14 days, and colonies counted.

Nuclear Fractionation and Chromatin Isolation. PCNA association with chromatin was evaluated, as previously published in Tan, *et al.* (Tan et al., 2012). MDA-MB-436 cells were plated,

Molecular Pharmacology Fast Forward. Published on December 5, 2014 as DOI: 10.1124/mol.114.093211
This article has not been copyedited and formatted. The final version may differ from this version.

treated with 30 μM R9-cc-caPeptide, and lysed in buffer A (10 mM Tris–HCl, pH 7.4, 2.5 mM $MgCl_2$, 0.5% NP-40, 1 mM DTT, 1 mM PMSF, and protease inhibitor cocktail). Samples were then pelleted by centrifugation (1500 x g, 2 min, 4°C), and the supernatant was collected as NP-40-extractable (NP-E) fraction. The pellet was washed in buffer B (10 mM Tris–HCl, pH 7.4, 150 mM NaCl, 1 mM PMSF, and a protease inhibitor cocktail), resuspended, and digested in buffer C (10 mM Tris–HCl, pH 7.4, 10 mM NaCl, 5 mM $MgCl_2$, 0.2 mM PMSF, and protease inhibitors) with 200 units/10^7 cells of DNase I for 30 min at 37°C. After centrifugation at 13,000 x g for 5 min at 4°C, the supernatant was collected as NP40 resistant (NP-R) fraction. NP-E and NP-R fractions of the protein were analyzed by western blot.

Animal Model. NOD/SCID/IL2R, gamma null (NSG) mice 4 - 6 weeks of age were produced from an in-house breeding colony. MDA-MB-436 cells were harvested, washed twice in PBS, and suspended in Matrigel (BD Biosciences, San Jose, CA) at 5 x 10^7/ml. 0.1 ml of suspended cells was injected into the mammary fat pads in the right flank of 20 mice. Seven days after tumor inoculation, mice were randomly grouped into three groups with 6 mice in each group. The mice were treated with PBS, R9-cc-srambled, or R9-cc-caPeptide 3 times a week via intratumoral injection. Tumor growth was measured weekly as well as at the end of the experiment by a dial caliper. Tumor volumes were estimated based on the length (L) and width (W) of the tumors ($V = L \times W^2 \times 0.5$). At the end of the experiment, tumors were isolated from sacrificed mice and their masses were measured. All experiments involving live animals were carried out in strict accordance with the recommendations in the Guide for the Care and Use of Laboratory Animals of the National Institutes of Health. This protocol (#11034) was reviewed and approved by the City of Hope Institutional Animal Care and Use Committee.

Molecular Pharmacology Fast Forward. Published on December 5, 2014 as DOI: 10.1124/mol.114.093211
This article has not been copyedited and formatted. The final version may differ from this version.

Results

Amino acids critical to caPCNA specificity are identified by sequence mapping of the caPCNAab. Commercially available antibodies used to identify PCNA are unable to distinguish between the normal PCNA (nmPCNA) and caPCNA isoforms (Malkas et al., 2006). The epitope these commercial antibodies (PC10 and C20) recognize spans amino acids 68-230 of PCNA, which are identical in both nmPCNA and caPCNA. In previous studies, we successfully developed a rabbit polyclonal antibody that specifically detects the caPCNA isoform through standard immunohistochemical (IHC) staining procedures. In order to identify the amino acid sequence that establishes caPCNA specificity, a series of rabbit polyclonal antibodies were produced by sequentially adding amino acids around the N- and C-terminus of the core region spanning amino acids 122-135 (listed in Figure 1A). The specificity of each antibody to caPCNA in MCF7 protein extract was then evaluated using 2-dimensional polyacrylamide gel electrophoresis (2-D PAGE), followed by Western blot analysis. As illustrated in Figure 1B, antibodies Ab125 (amino acids 125-133), Ab126 (amino acids 126-133), and Ab135 (amino acids 126-135) specifically recognize the caPCNA isoform. Antibodies composed of amino acids outside the 125-135 range resulted in a loss of specificity.

The results of the Western blot were then validated by immunohistochemical (IHC) staining of paraffin-embedded breast tissue samples. Both DCIS (ductal carcinoma in situ) and normal breast tissue samples were stained with the antibody panel. As shown in Figure 1C, PCNA is identified in each slide with a brown stain, and a darker brown indicates increased binding to the cell nuclei. Typically, IHC staining for breast cancer using the commercially available antibody to PCNA (PC10) will stain all proliferating cells expressing PCNA. The expression level correlates with the degree of proliferation, as shown in the lowest panel of

Molecular Pharmacology Fast Forward. Published on December 5, 2014 as DOI: 10.1124/mol.114.093211
This article has not been copyedited and formatted. The final version may differ from this version.

Figure 1C. In practice, this will not necessarily aid the pathologist in distinguishing between a normal proliferating cell and a cancer cell. When the samples shown in Figure 1C were stained with Ab 126 (126-133), the cancer cells in the DCIS sample exhibited nuclear staining of caPCNA, while the normal tissue samples do not stain with the antibody. Similar results were obtained with Ab 125 (125-135) and Ab 135 (126-135). Antibodies raised against amino acid sequences outside the 125-135 amino acid region were unable to differentiate between PCNA expressed in normal cells and caPCNA expressed in cancer cells. Amino acids 125-135, identified from both western blot analysis and IHC staining, represent the PCNA region unique to the cancer-associated isoform within the interdomain connector loop (IDCL) of PCNA. This is the region where numerous proteins required for proper DNA replication and repair interact with the PCNA molecule.

A peptide mimicking a portion of the interaction region is developed for efficient cellular uptake and is cytotoxic in a triple-negative breast cancer cell line. In a separate study conducted by Roos, *et al.*, monoclonal antibodies created from shorter sequences of PCNA exhibited the ability to inhibit *in vitro* DNA replication (Roos et al., 1996). The epitopal region used in those experiments spanned residues 121-135, which is located within the interdomain connector loop (IDCL) of PCNA. From our antibody scanning study, Ab 126 (recognizing amino acids 126-133) was selective for the caPCNA isoform expressed in cancer cells. Using this information, a peptide corresponding to PCNA amino acids 126-133 was synthesized (caPeptide) and tested for its therapeutic potential. One of the drawbacks in using peptides as therapeutics, however, is that most lack the polarity necessary to passively diffuse through the cell membrane. In order to aid in the uptake process, positively-charged chains, such as a series of arginines, lysines, or histidines, have been used previously. Polyarginines display the ability

Molecular Pharmacology Fast Forward. Published on December 5, 2014 as DOI: 10.1124/mol.114.093211
This article has not been copyedited and formatted. The final version may differ from this version.

to promote cellular uptake more efficiently than polylysines and polyhistidines (Deshayes et al., 2005; Wender et al., 2000). Detailed analyses of the polyarginine length indicate that a 9 arginine sequence is most effective for cellular penetration and uptake, with the sequence in "all-D" configuration to minimize proteolysis (Wender et al., 2000). Thus, for testing purposes, the caPeptide was linked to nine "D" arginine residues (R9-cc-caPeptide).

To establish the R9 sequence is necessary for efficient cellular uptake, 5-carboxyfluorescein (5-FAM) was attached to the N-terminus of the R9-cc-caPeptide. MDA-MB-436 cells were treated with 10 μM FAM-tagged R9-cc-caPeptide, and the uptake was monitored and imaged using fluorescence microscopy at two hour intervals for 12 hours, followed by imaging at 24 hours. MDA-MB-436 cells were derived from the pleural fluid of a 43 year old woman diagnosed with breast cancer (Brinkley et al., 1980). This particular cell line exhibits a triple negative, highly invasive breast cancer phenotype (Gordon et al., 2003). As illustrated in Figure 2A, FAM-labeled R9-cc-caPeptide enters MDA-MB-436 cells within 2 hours of treatment, and accumulates in these cells up to 24 hours. After 24 hours, the cells were washed with PBS and monitored for efflux of the peptide over the next 12 hours. FAM-labeled R9-cc-caPeptide remains in the cell up to 11 hours after the wash step (Figure 2A). To verify the accumulation observed is not due to a background effect of FAM tag alone, the MDA-MB-436 cells were treated with FAM tag only. As shown in Figure 2B, the FAM tag did not remain in the cells following the wash step as long as the FAM-tagged R9-cc-caPeptide, verifying the fluorescence observed was not due to FAM tag alone.

We then sought to verify cytotoxicity in MDA-MB-436 cells after R9-cc-caPeptide treatment. Increasing concentrations of the peptide were added to plated cells and analyzed using the CellTiter-Glo Luminescent Cell Viability Assay (Promega, Madison, WI). In this

Molecular Pharmacology Fast Forward. Published on December 5, 2014 as DOI: 10.1124/mol.114.093211
This article has not been copyedited and formatted. The final version may differ from this version.

approach used to measure cell viability, the luminescence measured is directly proportional to the amount of ATP produced by metabolically active cells. This measurement technique is reportedly the most sensitive cell-based assay for cytotoxicity (Petty et al., 1995). As shown in Figure 3A, R9-cc-caPeptide exhibited a dose-dependent response in these particular breast cancer cells (MDA-MB-436). The dose-response data was then analyzed using GraphPad Prism 5 to fit a sigmoidal dose response curve and determine the half maximal effective concentration (EC_{50}) of R9-cc-caPeptide. The EC_{50} determined from fit was approximately 28.8 μM, with 95% confidence interval 23.5 to 35.3 μM.

To confirm the specific sequence of the peptide is required for cytotoxic activity, a scrambled version of the caPeptide (R9-cc-scrambled) was constructed using the same eight amino acids randomly placed in a scrambled sequence. MDA-MB-436 cells were treated with up to 100 μM of both constructs for 48 hours and evaluated for viability using the MTT assay, as described in the Material and Methods section. As shown in Figure 3B, R9-cc-caPeptide treatment dose-dependently decreases cell viability. When MDA-MB-436 cells are treated with the R9-cc-scrambled construct, limited cellular toxicity was observed (Figure 3B). In addition, treatment of the peptide in D-configuration with an R9-cc-linkage (all-D) elicited a response similar to scrambled peptide treatment (Figure 3B). Both variations of the caPeptide (scrambled and all-D) confirmed the specific caPeptide sequence is critical to the observed cytotoxic action.

To further demonstrate the R9 sequence is an effective mechanism for delivery into the breast cancer cell line, treatment with the R9-cc-caPeptide construct was compared to the unlinked version (caPeptide). MDA-MB-436 cells were treated with up to 100 μM of caPeptide for 48 hours, and then evaluated for viability using the MTT assay. Figure 3B confirms that the R9 sequence is key to peptide delivery and cellular toxicity, as treatment with caPeptide alone

Molecular Pharmacology Fast Forward. Published on December 5, 2014 as DOI: 10.1124/mol.114.093211
This article has not been copyedited and formatted. The final version may differ from this version.

had no effect on the MDA-MB-436 cells. These cells were also treated with increasing concentrations of the R9-cc alone to establish that the nine arginines in D-configuration did not contribute to the observed cytotoxicity, and MTT analysis (Figure 3B) confirms this.

R9-cc-caPeptide targets caPCNA identified in cancer cells. After demonstrating the effectiveness of the R9-cc-caPeptide in treating the selected triple negative breast cancer cell line, we then sought to confirm the caPeptide targets the caPCNA that is prevalent in cancer cells. Therefore, we used a conventional normal immortalized breast cancer cell line (MCF10A) and primary human mammary epithelial cells (HMECs). Both cell types were treated with increasing concentrations of R9-cc-caPeptide, and the EC_{50} was evaluated. As shown in Figure 3C, the R9-cc-caPeptide is well tolerated by HMEC and MCF10A cells, with EC_{50} of 94 μM and greater than 100 μM, respectively, as compared to 28.8 μM in MDA-MB-436 cells. These results demonstrate that R9-cc-caPeptide treatment is more effective in cancer cells, and further confirms that the peptide preferentially targets PCNA-dependent interactions within cancer cells relative to those in non-cancer cells.

R9-cc-caPeptide induces apoptosis in triple-negative breast cancer cells. MDA-MB-436 cells ($1x10^6$ cells/sample) were treated with increasing concentrations of R9-cc-caPeptide for 24 hours, stained with Annexin V and propidium iodide (PI), and then analyzed using flow cytometry. After 24 hours of treatment, approximately 30% of the cells exhibited apoptosis (Annexin V positive, PI negative) when treated with 50 μM R9-cc-caPeptide (Figure 4A, Supplemental Figure 1). 100 μM R9-cc-caPeptide treatment results in approximately 20% of the cells becoming necrotic (Annexin V positive, PI positive) over the same time period. When treated with 100 μM of R9-cc-scrambled, less than 5% of cells undergo apoptosis. These results

Molecular Pharmacology Fast Forward. Published on December 5, 2014 as DOI: 10.1124/mol.114.093211
This article has not been copyedited and formatted. The final version may differ from this version.

correlate with previous studies showing the induction of apoptosis in neuroblastoma cells following R9-cc-caPeptide treatment (Zhang and Powell, 2005).

Staining was also performed in the nonmalignant cell lines (MCF10A and HMEC). As shown in Figure 4B, treatment of these cells with R9-cc-caPeptide resulted in little apoptotic staining above that of the control cells receiving either no treatment or treatment with R9-cc-scrambled. These results further confirm the specificity of R9-cc-caPeptide for inducing apoptosis in triple-negative breast cancer cells.

R9-cc-caPeptide treatment inhibits the clonogenicity of triple-negative breast cancer cells. MDA-MB-436 cells were treated with increasing concentrations of R9-cc-caPeptide or R9-scrambled peptide for 1 hour, and 750 treated cells were seeded in 10 cm culture dishes. As shown in Figure 5 (with images of representative plates in Supplemental Figure 2), the R9-cc-caPeptide treatment decreased the ability of the triple-negative breast cancer cells to form colonies in a dose-dependent manner. Treatment with approximately 40 μM of R9-cc-caPeptide resulted in a 50% decrease of clonogenicity. Treatment with increasing concentrations of R9-cc-scrambled had little or no effect on the ability of cells to form colonies. This result is consistent with the previous cytotoxicity experiments (Figures 3 and 4).

R9-cc-caPeptide inhibits PCNA association to chromatin. In addition to interacting with DNA replication and repair molecules, PCNA is essential in chromatin association. Previous studies have demonstrated that PCNA interacts with both chromatin assembly factor-1 (CAF-1) and replicating factor C (RF-C) during chromatin assembly (Moggs et al., 2000; Shibahara and Stillman, 1999; Tan et al., 2012). CAF-1 has been shown to interact with PCNA within the region of interest (IDCL) (Moggs et al., 2000). Previous studies have shown that the

Molecular Pharmacology Fast Forward. Published on December 5, 2014 as DOI: 10.1124/mol.114.093211
This article has not been copyedited and formatted. The final version may differ from this version.

inhibition of PCNA accumulation in chromatin correlates with the level of cytotoxicity observed in cells (Tan et al., 2012). We therefore wanted to assess whether treatment of cells with R9-cc-caPeptide alters the association of PCNA with chromatin. MDA-MB-436 cells were treated with 30 μM of R9-cc-caPeptide for 8 hours, then separated into NP-40 extractable (E) and resistant (R) fractions. As shown in Figure 6, treatment of cells with R9-cc-caPeptide decreases the association of PCNA with chromatin in cells (NP-R). This establishes R9-cc-caPeptide's ability to block the interaction of PCNA with chromatin-associated proteins, such as CAF-1.

R9-cc-caPeptide inhibits tumor growth in a mouse model. Because R9-cc-caPeptide exhibits therapeutic potential in a number of *in vitro* assays using triple-negative breast cancer cells, we then sought to recapitulate this anti-cancer activity using an *in vivo* breast cancer model. We tested R9-cc-caPeptide in NSG mice bearing xenograft tumors derived from MDA-MB-436 cells and found that R9-cc-caPeptide significantly and almost completely inhibited tumor growth as assessed by measuring the tumor volume (Figure 7A) and final mass (Figure 7B) in comparison to the control groups that were treated with either PBS or R9-cc-scrambled. These *in vivo* results correlate with our *in vitro* results and further validate the therapeutic potential of targeting the PCNA region (L126-Y133) as a novel approach in treating triple-negative breast cancer.

Various cancer cell types exhibit a range of sensitivity to R9-cc-caPeptide treatment. The cytotoxicity of R9-cc-caPeptide was tested in an ER+ breast cancer cell line (MCF 7), along with two other cancer cell types, lymphoma (U937) and pancreatic (PaCa-2). MTT analysis of each cell line treated with R9-cc-caPeptide is illustrated in Figure 8A. The pancreatic cancer cell line exhibited increased sensitivity to R9-cc-caPeptide treatment (EC_{50} of 16 μM), as compared to lymphoma (30 μM), and the two breast cancer cell lines (28 μM for MDA-MB-436 and 60 μM

Molecular Pharmacology Fast Forward. Published on December 5, 2014 as DOI: 10.1124/mol.114.093211
This article has not been copyedited and formatted. The final version may differ from this version.

for MCF 7). The varying cytotoxic efficacy of the R9-cc-caPeptide on the various cancer cell lines tested may be related to alterations within the DNA replication and repair machinery that are inherent to different types of cancers or the increased uptake or reduced efflux of the peptide in different cell types. Cell lines exhibiting greater resistance to the peptide treatment may be more dependent on other repair pathways that do not require PCNA interaction. Further examination of the specificity of the peptide sequence for different PCNA-interacting proteins and enzymes within the DNA replication and repair process are currently under way.

R9-cc-caPeptide contributes to synthetic lethality in BRCA-deficient breast cancer cells. BRCA1 has been identified as a critical tumor suppressor gene in breast cancer, and loss-of-function mutations confer up to an 82% risk of developing breast cancer by the age of 80 (King et al., 2003). BRCA1 is a 220 kDa nuclear phosphoprotein containing several functional domains that are able to interact with various proteins involved in DNA damage repair pathways. In response to DNA damage, BRCA1 participates in homologous recombination by forming a complex with BRCA2, RAD51, and PCNA (Gilmore et al., 2003; Karran, 2000). BRCA1 may also be involved in non-homologous end joining (NHEJ), a less accurate repair pathway, by aligning short areas of base homology on either side of the DNA break before ligation (Zhong et al., 2002). BRCA1-deficient cells exhibit increased genomic instability, and this is most likely due to an inability to respond appropriately to DNA damage. This ultimately results in the accumulation of DNA damage (Zhang and Powell, 2005). In the absence of BRCA1, these repair pathways are rendered ineffective, increasing the toxicity of DNA damaging agents (Kennedy et al., 2004).

As shown in Figure 8B, HCC 1937 cells expressing a fuctional BRCA1 transgene (HCC 1937 BRCA+) are more resistant to increased R9-cc-caPeptide treatment; an IC_{50} of 90 μM was

Molecular Pharmacology Fast Forward. Published on December 5, 2014 as DOI: 10.1124/mol.114.093211
This article has not been copyedited and formatted. The final version may differ from this version.

determined in BRCA+ cells, as compared to an IC_{50} of 60 μM in the BRCA-deficient HCC 1937 cells. Previous investigations have shown that these BRCA-deficient HCC 1937 cells are increasingly more sensitive to conventional DNA damaging agents, such as cisplatin (Bayraktar and Gluck, 2012; Tassone et al., 2003). The results shown in Figure 8B correlate with these observations, and this helps to confirm that the R9-cc-caPeptide has the ability to disrupt protein functions critical to DNA repair in cancer cells, especially those that require specific PCNA-dependent repair pathways for survival.

Specific amino acids within the caPeptide sequence are critical to the observed cytotoxicity. To further characterize the specific mechanism of interaction of the caPeptide contributing to cytotoxicity, peptide constructs, each containing a single alanine substitution within the peptide sequence, were synthesized (Figure 9A). MDA-MB-436 cells ($1x10^6$) were individually treated with 75 μM of each of the R9-cc-alanine substituted caPeptide for 24 hours, and then analyzed using flow cytometry. The calculated % cell death of each R9-linked peptide is shown in Figure 9A.

If a critical amino acid is substituted by an alanine, treatment with that particular peptide would presumably be less cytotoxic in cells, as compared to the original (R9-cc-caPeptide). Alanine substitution of an amino acid not critical to the protein-protein interactions, however, should not affect the observed cytotoxicity. Representative FACS data for each type of response is shown in Supplemental Figure 3. As illustrated in Figure 9A, alanine substitution at amino acid 126, 128, 130, 132, and 133 virtually eliminated the cytotoxicity of the peptide, and thus the native amino acids (leucine, isoleucine, glutamic acids, and tyrosine, respectively) are therefore likely critical to the activity of the peptide. Alanine substitution at amino acid 127 and 129 exhibited little or no change in the observed cytotoxicity of the peptide, and thus the native

Molecular Pharmacology Fast Forward. Published on December 5, 2014 as DOI: 10.1124/mol.114.093211
This article has not been copyedited and formatted. The final version may differ from this version.

amino acids (glycine and proline, respectively) most likely do not contribute to cytotoxicity. Interestingly, an alanine substitution at amino acid 131 increased cytotoxicity of the peptide. This indicates the R9-cc-Q131A is potentially a better therapeutic. Further studies are currently underway to investigate this phenomenon.

Molecular Pharmacology Fast Forward. Published on December 5, 2014 as DOI: 10.1124/mol.114.093211
This article has not been copyedited and formatted. The final version may differ from this version.

Discussion

As previously described, PCNA plays an integral role in DNA replication and repair. Therefore, if the PCNA function is altered in cancer cells, there is a greater potential for error propagation within the DNA structure itself. A characteristic common to cancer is accumulation of these mutations during the replication process, generating genomic instability within the cell. According to the "mutator phenotype" hypothesis, as DNA begins to replicate with less fidelity in cells, errors accumulate, and the cells take on a "mutator phenotype", eventually leading to the incidence of cancer (Loeb, 1998, 2001, 2010). Although the actual driving force behind this loss of DNA replication fidelity has yet to be determined, it is very possible that a malfunction within the replication machinery itself is the main cause of error propagation.

In the previous communication (Malkas et al., 2006), we had successfully developed a rabbit polyclonal antibody that specifically detects the cancer-associated isoform of PCNA (caPCNAab). This antibody has now been validated through both Western blot analysis of breast cancer cell extracts and immunohistochemical (IHC) staining of breast tissue samples. Figure 1 demonstrates its specificity to the caPCNA isoform expressed in cancer cells and defines the cancer-selective epitope of the PCNA sequence (amino acids 125-135). From these findings, we then developed a peptide mimicking this caPCNA-specific region. This peptide exhibits the ability to compete with the binding of accessory proteins to caPCNA, thereby targeting cells containing caPCNA, inhibiting DNA replication, and eventually leading to cellular apoptosis.

The caPeptide sequence alone was incubated in MDA-MB-436 cells for 48 hours in concentrations up to 100 μM, but no cytotoxicity was observed (Figure 3B). Because most

Molecular Pharmacology Fast Forward. Published on December 5, 2014 as DOI: 10.1124/mol.114.093211
This article has not been copyedited and formatted. The final version may differ from this version.

peptides cannot passively diffuse into cells, a linker of nine arginines in the "D"- configuration was attached to the N-terminus of the peptide to create R9-cc-caPeptide. Treatment of MDA-MB-436 cells with fluorescently-tagged R9-cc-caPeptide demonstrated sufficient cellular uptake and accumulation of the peptide (Figure 2). Subsequent rinsing of the cells (efflux) showed the R9-cc-caPeptide remained in the cells beyond 12 hours. Treatment of MDA-MB-436 cells with increasing concentrations of R9-cc-caPeptide up to 100 μM resulted in dose-dependent cell killing, and the EC_{50} determined for MDA-MB-436 cells was approximately 30 μM (Figure 3A). As a control, cells treated with a scrambled peptide attached to the nonaarginine (R9-cc-scrambled) or the all-D peptide exhibited little cytotoxicity. The study also confirmed the importance of R9 for cellular uptake and the specificity of the caPeptide sequence for cytotoxic action. The specificity of the peptide for cells containing caPCNA was further demonstrated, as R9-cc-caPeptide exhibited limited cytotoxicity in the nonmalignant cell lines (MCF10A and HMECs) (Figures 3C and 4B).

The cell line chosen for preliminary experiments with the caPeptide, MDA-MB-436, is a triple negative breast cancer cell line. Treatment with R9-cc-caPeptide was shown to decrease cell viability through the measurement of ATP, flow cytometry, and clonogenic assays. It can also inhibit PCNA accumulation in chromatin. Peptide cytotoxicity was subsequently tested in two other cancer cell lines (lymphoma (U937) and pancreatic cancer (PaCa-2)), and breast cancers of different genetic makeup (HCC 1937 and MCF 7). The results demonstrate that the R9-cc-caPeptide displays cytotoxicity in various forms of cancer. Furthermore, the preliminary data from the *in vivo* mouse model that the R9-cc-caPeptide may have potential as a therapeutic agent.

Molecular Pharmacology Fast Forward. Published on December 5, 2014 as DOI: 10.1124/mol.114.093211
This article has not been copyedited and formatted. The final version may differ from this version.

Existing X-ray crystallography data on the interaction site within PCNA was utilized to aid in visualizing the relationship between the observed cytotoxicity and specific amino acids within the peptide sequence that affect interactions with PCNA binding partners. The binding model shown in Figure 9B is a reproduction of PCNA interacting with FEN-1 using previously published X-ray crystallography (PDB ID 1UL1, Sakurai et al., 2005). The C-terminal (aa330-380) of the FEN-1 molecule forms the "plug" that fits into the IDCL pocket of the PCNA molecule. Closer examination shows that the PCNA peptide region encompassing aa126-133 does, in fact, form a cavity for the FEN-1 molecule to bind. Amino acids 126 and 133 are positioned above the cavity in such a way to presumably provide complementary van der Waals interactions between FEN-1 and PCNA. As demonstrated by alanine mutation analysis (Figure 9A), substitution of these amino acids with an alanine resulted in a decrease of the cytotoxic activity, confirming their importance to the interaction. The model also reveals that amino acids 127 and 132 face away from the pocket and do not appear to be involved in the PCNA/FEN-1 interaction, correlating with the alanine mutation analysis. The nonpolar valine at residue 346 makes contact with the hydrophobic leucine at residue 126 on PCNA. Our mutational studies confirm that the replacement of either the leucine (126) or the tyrosine (133) with an alanine results in the loss of key protein interactions within the IDCL, thereby reducing the mimicking capability of the peptide. Previous work in the lab confirms that the caPeptide sequence interferes with FEN1 binding to PCNA, as demonstrated by surface plasmon resonance (SPR) and immunofluorescence (Zhang and Powell, 2005).

Although only the interaction between FEN-1 and PCNA was applied to the current study, the cavity formed by PCNA aa126-133 is a binding site for a variety of other binding partners (Bowman et al., 2004; Bruning and Shamoo, 2004; Chapados et al., 2004; Gulbis et al.,

1996; Kontopidis et al., 2005; Sakurai et al., 2005; Vijayakumar et al., 2007). PCNA affinity column elution studies have confirmed the role of PCNA in linking DNA replication and cell cycle control of DNA replication via protein-protein interactions (Loor et al., 1997). Peptides identified as interacting with PCNA in this format include pol δ (125 kDa subunit), pol ε (145 kDa subunit), RFC (subunits 37 and 40), RPA (subunits 70, 34, and 11), DNA helicase II, and topoisomerase I. Each of these proteins contains a PIP-box that interacts with the pocket region formed in the IDCL of the PCNA molecule. Although there are many other amino acid interacting points between PCNA and its binding partners, the cavity formed in part by the caPeptide region is necessary for proper binding and the initiation of the cellular processes produced by the interaction.

Other studies involving a combination of the crystal structure and experimental techniques describe PCNA interaction with other proteins. X-ray crystallography of p21-PCNA interactions correlate with the flow cytometry results in this study (Figure 9A). The crystal structure of p21 complexed with PCNA revealed major interactions with residues leucine-126, isoleucine-128, and tyrosine-133 of the PCNA IDCL (Gibbs et al., 1997). The hydroxyl group of tyrosine-151 of the p21 peptide forms a hydrogen bond with glutamine-131 and forms an ordered water pair with tyrosine-133 of PCNA (Pascal et al., 2006). When PCNA is mutated with an alanine at the isoleucine residue (position 128), pol δ is unable to bind, resulting in a loss of processivity (Zhang et al., 1998). This correlates with our flow cytometry data of the I128A mutant, where cytotoxicity is virtually eliminated by this alanine substitution. The affinity for pol δ presumably decreases, rendering it ineffective. These results further confirm the caPeptide has the ability to disrupt the proper functioning of pol δ. This type of disruption is important, as PCNA has been shown to stimulate pol δ processivity by decreasing the dissociation of pol δ

Molecular Pharmacology Fast Forward. Published on December 5, 2014 as DOI: 10.1124/mol.114.093211
This article has not been copyedited and formatted. The final version may differ from this version.

from the template-primer complex (McConnell et al., 1996), while moderately increasing the rate of incorporation of a single nucleotide (Ng et al., 1991). PCNA can enhance pol δ activity across DNA damage sites that include a model abasic site (modified tetrahydrofuran), 8-oxo-dG, AF-dG (Mozzherin et al., 1997), and thymine dimers (a common DNA photoproduct) (O'Day et al., 1992).

As mentioned previously, the caPeptide designed for these studies is derived from a portion of the flexible IDCL region of PCNA. This particular region of PCNA is considered to have a disordered structure (Bruning and Shamoo, 2004). Disordered regions in proteins indicate the locations for protein-protein interaction. The cytotoxicity observed with R9-cc-caPeptide treatment suggests that the peptide has the ability to compete with PCNA for its binding partners, thereby inhibiting their binding ability and proper functioning in normal DNA replication and repair processes.

Molecular Pharmacology Fast Forward. Published on December 5, 2014 as DOI: 10.1124/mol.114.093211
This article has not been copyedited and formatted. The final version may differ from this version.

Acknowledgments

From City of Hope, we thank Drs. Hongzhi Li and Yate-Ching Yuan (Director) in the Bioinformatics for their assistance in the illustration of the X-ray crystallography data, and Lucy Brown (Manager) and her staff in the Analytical Cytometry Core for their assistance with the alanine scanning data. We also thank Dr. Fei Shen at Indiana University for conducting the peptide uptake and retention studies. Finally, we thank Angelica Ruiz for her assistance in the preparation of this manuscript.

Authorship Contributions

Participated in research design: Smith, Phipps, Dobrolecki, Mabrey, Chen, Gu, Ann, Hickey, Malkas.

Conducted experiments: Smith, Phipps, Dobrolecki, Mabrey, Gulley, Dillehay, Chen, Gu, Hickey.

Contributed new reagents or analytic tools: Dobrolecki, Mabrey, Dillehay, Dong, Fields, Ann.

Performed data analysis: Smith, Dobrolecki, Mabrey, Gulley, Dillehay, Dong, Chen, Gu, Hickey.

Wrote the manuscript: Smith.

Contributed the writing of the manuscript: Chen, Fields, Gu, Hickey, Malkas.

Molecular Pharmacology Fast Forward. Published on December 5, 2014 as DOI: 10.1124/mol.114.093211
This article has not been copyedited and formatted. The final version may differ from this version.

References

Bayraktar, S., and Gluck, S. (2012). Systemic therapy options in BRCA mutation-associated breast cancer. Breast Cancer Res Treat *135*, 355-366.

Bechtel, P.E., Hickey, R.J., Schnaper, L., Sekowski, J.W., Long, B.J., Freund, R., Liu, N., Rodriguez-Valenzuela, C., and Malkas, L.H. (1998). A unique form of proliferating cell nuclear antigen is present in malignant breast cells. Cancer Research *58*, 3264-3269.

Bowman, G.D., O'Donnell, M., and Kuriyan, J. (2004). Structural analysis of a eukaryotic sliding DNA clamp-clamp loader complex. Nature *429*, 724-730.

Brinkley, B.R., Beall, P.T., Wible, L.J., Mace, M.L., Turner, D.S., and Cailleau, R.M. (1980). Variations in cell form and cytoskeleton in human breast carcinoma cells in vitro. Cancer Res *40*, 3118-3129.

Bruning, J.B., and Shamoo, Y. (2004). Structural and thermodynamic analysis of human PCNA with peptides derived from DNA polymerase-delta p66 subunit and flap endonuclease-1. Structure *12*, 2209-2219.

Chapados, B.R., Hosfield, D.J., Han, S., Qiu, J., Yelent, B., Shen, B., and Tainer, J.A. (2004). Structural basis for FEN-1 substrate specificity and PCNA-mediated activation in DNA replication and repair. Cell *116*, 39-50.

Chu, J.S., Huang, C.S., and Chang, K.J. (1998). Proliferating cell nuclear antigen (PCNA) immunolabeling as a prognostic factor in invasive ductal carcinoma of the breast in Taiwan. Cancer Lett *131*, 145-152.

Deshayes, S., Morris, M.C., Divita, G., and Heitz, F. (2005). Cell-penetrating peptides: tools for intracellular delivery of therapeutics. Cell Mol Life Sci *62*, 1839-1849.

Garg, P., and Burgers, P.M. (2005). Ubiquitinated proliferating cell nuclear antigen activates translesion DNA polymerases eta and REV1. Proc Natl Acad Sci U S A *102*, 18361-18366.

Gibbs, E., Kelman, Z., Gulbis, J.M., O'Donnell, M., Kuriyan, J., Burgers, P.M., and Hurwitz, J. (1997). The influence of the proliferating cell nuclear antigen-interacting domain of p21(CIP1) on DNA synthesis catalyzed by the human and Saccharomyces cerevisiae polymerase delta holoenzymes. J Biol Chem *272*, 2373-2381.

Gilmore, P.M., Quinn, J.E., Mullan, P.B., Andrews, H.N., McCabe, N., Carty, M., Kennedy, R.D., and Harkin, D.P. (2003). Role played by BRCA1 in regulating the cellular response to stress. Biochem Soc Trans *31*, 257-262.

Gordon, L.A., Mulligan, K.T., Maxwell-Jones, H., Adams, M., Walker, R.A., and Jones, J.L. (2003). Breast cell invasive potential relates to the myoepithelial phenotype. Int J Cancer *106*, 8-16.

Gulbis, J.M., Kelman, Z., Hurwitz, J., O'Donnell, M., and Kuriyan, J. (1996). Structure of the C-terminal region of p21(WAF1/CIP1) complexed with human PCNA. Cell *87*, 297-306.

Hoege, C., Pfander, B., Moldovan, G.L., Pyrowolakis, G., and Jentsch, S. (2002). RAD6-dependent DNA repair is linked to modification of PCNA by ubiquitin and SUMO. Nature *419*, 135-141.

Hoelz, D.J., Arnold, R.J., Dobrolecki, L.E., Abdel-Aziz, W., Loehrer, A.P., Novotny, M.V., Schnaper, L., Hickey, R.J., and Malkas, L.H. (2006). The discovery of labile methyl esters on proliferating cell nuclear antigen by MS/MS. Proteomics *6*, 4808-4816.

Kannouche, P.L., and Lehmann, A.R. (2004). Ubiquitination of PCNA and the polymerase switch in human cells. Cell Cycle *3*, 1011-1013.

Kannouche, P.L., Wing, J., and Lehmann, A.R. (2004). Interaction of human DNA polymerase eta with monoubiquitinated PCNA: a possible mechanism for the polymerase switch in response to DNA damage. Mol Cell *14*, 491-500.

Karran, P. (2000). DNA double strand break repair in mammalian cells. Curr Opin Genet Dev *10*, 144-150.

Kemp, P.v.d., Padula, M.d., Burguiere-Slezak, G., Ulrich, H., and Boiteux, S. (2009). PCNA monoubiquitylation and DNA polymerase eta ubiquitin-binding domain are required to prevent.

Kennedy, R.D., Quinn, J.E., Mullan, P.B., Johnston, P.G., and Harkin, D.P. (2004). The role of BRCA1 in the cellular response to chemotherapy. J Natl Cancer Inst *96*, 1659-1668.

King, M.C., Marks, J.H., and Mandell, J.B. (2003). Breast and ovarian cancer risks due to inherited mutations in BRCA1 and BRCA2. Science *302*, 643-646.

Kontopidis, G., Wu, S.Y., Zheleva, D.I., Taylor, P., McInnes, C., Lane, D.P., Fischer, P.M., and Walkinshaw, M.D. (2005). Structural and biochemical studies of human proliferating cell nuclear antigen complexes provide a rationale for cyclin association and inhibitor design. Proc Natl Acad Sci U S A *102*, 1871-1876.

Krijger, P.H., van den Berk, P.C., Wit, N., Langerak, P., Jansen, J.G., Reynaud, C.A., de Wind, N., and Jacobs, H. (2011). PCNA ubiquitination-independent activation of polymerase eta during somatic hypermutation and DNA damage tolerance. DNA Repair (Amst) *10*, 1051-1059.

Loeb, L.A. (1998). Cancer cells exhibit a mutator phenotype. Adv Cancer Res *72*, 25-56.

Loeb, L.A. (2001). A mutator phenotype in cancer. Cancer Research *61*, 3230-3239.

Loeb, L.A. (2010). Mutator phenotype in cancer: origin and consequences. Semin Cancer Biol *20*, 279-280.

Loor, G., Zhang, S.J., Zhang, P., Toomey, N.L., and Lee, M.Y. (1997). Identification of DNA replication and cell cycle proteins that interact with PCNA. Nucleic Acids Res *25*, 5041-5046.

Malkas, L.H., Herbert, B.S., Abdel-Aziz, W., Dobrolecki, L.E., Liu, Y., Agarwal, B., Hoelz, D., Badve, S., Schnaper, L., Arnold, R.J.*, et al.* (2006). A cancer-associated PCNA expressed in breast cancer has implications as a potential biomarker. Proc Natl Acad Sci U S A *103*, 19472-19477.

McConnell, M., Miller, H., Mozzherin, D.J., Quamina, A., Tan, C.K., Downey, K.M., and Fisher, P.A. (1996). The mammalian DNA polymerase delta--proliferating cell nuclear antigen--template-primer complex: molecular characterization by direct binding. Biochemistry *35*, 8268-8274.

Moggs, J.G., Grandi, P., Quivy, J.P., Jonsson, Z.O., Hubscher, U., Becker, P.B., and Almouzni, G. (2000). A CAF-1-PCNA-mediated chromatin assembly pathway triggered by sensing DNA damage. Mol Cell Biol *20*, 1206-1218.

Mozzherin, D.J., Shibutani, S., Tan, C.K., Downey, K.M., and Fisher, P.A. (1997). Proliferating cell nuclear antigen promotes DNA synthesis past template lesions by mammalian DNA polymerase delta. Proc Natl Acad Sci U S A *94*, 6126-6131.

Naryzhny, S.N., and Lee, H. (2004). The post-translational modifications of proliferating cell nuclear antigen: acetylation, not phosphorylation, plays an important role in the regulation of its function. J Biol Chem *279*, 20194-20199.

Ng, L., Tan, C.K., Downey, K.M., and Fisher, P.A. (1991). Enzymologic mechanism of calf thymus DNA polymerase delta. J Biol Chem *266*, 11699-11704.

O'Day, C.L., Burgers, P.M., and Taylor, J.S. (1992). PCNA-induced DNA synthesis past cis-syn and trans-syn-I thymine dimers by calf thymus DNA polymerase delta in vitro. Nucleic Acids Res *20*, 5403-5406.

Pascal, J.M., Tsodikov, O.V., Hura, G.L., Song, W., Cotner, E.A., Classen, S., Tomkinson, A.E., Tainer, J.A., and Ellenberger, T. (2006). A flexible interface between DNA ligase and PCNA supports conformational switching and efficient ligation of DNA. Mol Cell *24*, 279-291.

Petty, R.D., Sutherland, L.A., Hunter, E.M., and Cree, I.A. (1995). Comparison of MTT and ATP-based assays for the measurement of viable cell number. J Biolumin Chemilumin *10*, 29-34.

Prosperi, E. (1997). Multiple roles of the proliferating cell nuclear antigen: DNA replication, repair and cell cycle control. Prog Cell Cycle Res *3*, 193-210.

Punchihewa, C., Inoue, A., Hishiki, A., Fujikawa, Y., Connelly, M., Evison, B., Shao, Y., Heath, R., Kuraoka, I., Rodrigues, P., *et al.* (2012). Identification of small molecule proliferating cell nuclear antigen (PCNA) inhibitor that disrupts interactions with PIP-box proteins and inhibits DNA replication. J Biol Chem *287*, 14289-14300.

Roos, G., Jiang, Y., Landberg, G., Nielsen, N.H., Zhang, P., and Lee, M.Y. (1996). Determination of the epitope of an inhibitory antibody to proliferating cell nuclear antigen. Exp Cell Res *226*, 208-213.

Sabbioneda, S., Gourdin, A.M., Green, C.M., Zotter, A., Giglia-Mari, G., Houtsmuller, A., Vermeulen, W., and Lehmann, A.R. (2008). Effect of proliferating cell nuclear antigen ubiquitination and chromatin structure on the dynamic properties of the Y-family DNA polymerases. Mol Biol Cell *19*, 5193-5202.

Sakurai, S., Kitano, K., Yamaguchi, H., Hamada, K., Okada, K., Fukuda, K., Uchida, M., Ohtsuka, E., Morioka, H., and Hakoshima, T. (2005). Structural basis for recruitment of human flap endonuclease 1 to PCNA. EMBO J *24*, 683-693.

Sandoval, J.A., Hickey, R.J., and Malkas, L.H. (2005). Isolation and characterization of a DNA synthesome from a neuroblastoma cell line. J Pediatr Surg *40*, 1070-1077.

Sekowski, J.W., Malkas, L.H., Schnaper, L., Bechtel, P.E., Long, B.J., and Hickey, R.J. (1998). Human breast cancer cells contain an error-prone DNA replication apparatus. Cancer Research *58*, 3259-3263.

Shibahara, K., and Stillman, B. (1999). Replication-dependent marking of DNA by PCNA facilitates CAF-1-coupled inheritance of chromatin. Cell *96*, 575-585.

Stelter, P., and Ulrich, H.D. (2003). Control of spontaneous and damage-induced mutagenesis by SUMO and ubiquitin conjugation. Nature *425*, 188-191.

Tahan, S.R., Neuberg, D.S., Dieffenbach, A., and Yacoub, L. (1993). Prediction of early relapse and shortened survival in patients with breast cancer by proliferating cell nuclear antigen score. Cancer *71*, 3552-3559.

Tan, Z., Wortman, M., Dillehay, K.L., Seibel, W.L., Evelyn, C.R., Smith, S.J., Malkas, L.H., Zheng, Y., Lu, S., and Dong, Z. (2012). Small Molecule Targeting of PCNA Chromatin Association Inhibits Tumor Cell Growth. Mol Pharmacol.

Tassone, P., Tagliaferri, P., Perricelli, A., Blotta, S., Quaresima, B., Martelli, M.L., Goel, A., Barbieri, V., Costanzo, F., Boland, C.R., *et al.* (2003). BRCA1 expression modulates chemosensitivity of BRCA1-defective HCC1937 human breast cancer cells. Br J Cancer *88*, 1285-1291.

Venturi, A., Piaz, F.D., Giovannini, C., Gramantieri, L., Chieco, P., and Bolondi, L. (2008). Human hepatocellular carcinoma expresses specific PCNA isoforms: an in vivo and in vitro evaluation. Lab Invest *88*, 995-1007.

Vijayakumar, S., Chapados, B.R., Schmidt, K.H., Kolodner, R.D., Tainer, J.A., and Tomkinson, A.E. (2007). The C-terminal domain of yeast PCNA is required for physical and functional interactions with Cdc9 DNA ligase. Nucleic Acids Res *35*, 1624-1637.

Wang, S.C., Nakajima, Y., Yu, Y.L., Xia, W., Chen, C.T., Yang, C.C., McIntush, E.W., Li, L.Y., Hawke, D.H., Kobayashi, R., *et al.* (2006). Tyrosine phosphorylation controls PCNA function through protein stability. Nat Cell Biol *8*, 1359-1368.

Wang, X., Hickey, R.J., Malkas, L.H., Koch, M.O., Li, L., Zhang, S., Sandusky, G.E., Grignon, D.J., Eble, J.N., and Cheng, L. (2011). Elevated Expression of Cancer-Associated Proliferating Cell Nuclear Antigen in High-Grade Prostatic Intraepithelial Neoplasia and Prostate Cancer. The Prostate *71*, 7.

Warbrick, E. (2006). A functional analysis of PCNA-binding peptides derived from protein sequence, interaction screening and rational design. Oncogene *25*, 2850-2859.

Watanabe, K., Tateishi, S., Kawasuji, M., Tsurimoto, T., Inoue, H., and Yamaizumi, M. (2004). Rad18 guides poleta to replication stalling sites through physical interaction and PCNA monoubiquitination. EMBO J *23*, 3886-3896.

Wender, P.A., Mitchell, D.J., Pattabiraman, K., Pelkey, E.T., Steinman, L., and Rothbard, J.B. (2000). The design, synthesis, and evaluation of molecules that enable or enhance cellular uptake: peptoid molecular transporters. Proc Natl Acad Sci U S A *97*, 13003-13008.

Zhang, J., and Powell, S.N. (2005). The role of the BRCA1 tumor suppressor in DNA double-strand break repair. Mol Cancer Res *3*, 531-539.

Zhang, P., Sun, Y., Hsu, H., Zhang, L., Zhang, Y., and Lee, M.Y. (1998). The interdomain connector loop of human PCNA is involved in a direct interaction with human polymerase delta. J Biol Chem *273*, 713-719.

Zheleva, D.I., Zhelev, N.Z., Fischer, P.M., Duff, S.V., Warbrick, E., Blake, D.G., and Lane, D.P. (2000). A quantitative study of the in vitro binding of the C-terminal domain of p21 to PCNA: affinity, stoichiometry, and thermodynamics. Biochemistry *39*, 7388-7397.

Zhong, Q., Chen, C.F., Chen, P.L., and Lee, W.H. (2002). BRCA1 facilitates microhomology-mediated end joining of DNA double strand breaks. J Biol Chem *277*, 28641-28647.

Molecular Pharmacology Fast Forward. Published on December 5, 2014 as DOI: 10.1124/mol.114.093211
This article has not been copyedited and formatted. The final version may differ from this version.

Footnotes

This work was supported by the Department of Defense [Grant W81XWH-11-1-0786 to LHM]; and by the National Institutes of Health National Cancer Institute [Grants R01 CA121289 and P30CA033572]. The content is solely the responsibility of the authors and does not necessarily represent the official views of the National Institutes of Health.

Molecular Pharmacology Fast Forward. Published on December 5, 2014 as DOI: 10.1124/mol.114.093211
This article has not been copyedited and formatted. The final version may differ from this version.

Figure Legends

Figure 1 The epitope specific to cancer-associated PCNA (caPCNA) is identified by an overlapping peptide scan. (A) Rabbit polyclonal antibodies listed were generated from various overlapping PCNA amino acid sequences within the interdomain connector loop (IDCL) of PCNA. **(B)** Two-dimensional SDS-PAGE of an MCF7 S3 protein fraction followed by Western blotting (see Methods) was performed using each affinity purified antibody. PC10 was diluted 1:2000; Ab122 through Ab163 were diluted 1:500. Specificity of the antibody for caPCNA expressed by cancer cells was previously described in Malkas, et al. (Malkas et al., 2006). **(C)** Paraffin-embedded breast tissue samples were stained with the antibody series using immunohisochemical (IHC) staining techniques, as detailed in the Methods section.

Figure 2 The addition of a 9 D-arginine (R9-) sequence to caPeptide aids in uptake and efflux in breast cancer cells. (A) MDA-MB-436 cells were treated with fluorescein labeled R9-cc-caPeptide for 24 hours and the uptake was monitored. Cells were subsequently washed, and efflux of the fluorescein labeled R9-cc-caPeptide was monitored for 11 hours. **(B)** As a control, MDA-MB-436 cells were treated with fluorescein alone for 24 hours, and efflux was monitored for 7 hours.

Figure 3 The caPeptide sequence is required for cytotoxicity in MDA-MB-436 cells and targets caPCNA in cancer cells. (A) Exponentially growing ($3x10^3$) MDA-MB-436 cells were treated with increasing concentrations of R9-cc-caPeptide for 48 hours. Cell viability (Cell-Titer Glo assay) was evaluated as detailed in the Materials and Methods section of this paper. Activity was calculated as % of cells killed at each concentration, normalized to untreated MDA-MB-436 cells (control). 100% activity refers to 100% cell death. EC_{50} with 95% confidence was evaluated using non-linear regression in GraphPad Prism 5. **(B)** Exponentially growing MDA-MB-436 ($5x10^3$) cells were treated with increasing concentrations of caPeptide, R9-cc, R9-cc-scrambled, R9-cc-caPeptide, and R9-cc-caPeptide (D-form) for 48 hours. Cell proliferation (from MTT analysis) was evaluated as % of control cells (% Control), as detailed in the Materials and Methods section. **(C)** Exponentially growing MDA-MB-436, MCF10A, and human mammary epithelial cells (HMECs) were treated with increasing concentrations of R9-cc-caPeptide for 48 hours. Cell viability (Cell-Titer Glo assay) was evaluated as detailed in the Materials and Methods section of this paper. Activity was calculated as % of cells killed at each concentration, normalized to untreated MDA-MB-436 cells (control). EC_{50} was evaluated using non-linear regression in GraphPad Prism 5. Data points are means ($\pm$ S.D.) of octuplicate determinations in a representative experiment; similar results were obtained in at least three additional experiments.

Figure 4 Treatment of MDA-MB-436 cells with R9-cc-caPeptide results in cytotoxicity via apoptosis. Exponentially growing ($1x10^6$) MDA-MB-436 **(A, B)**, MCF10A **(B)**, and HMECs **(B)** cells were treated with increasing concentrations of R9-cc-caPeptide or 100 μM R9-cc-scrambled up to 24 hours. Annexin V staining was then evaluated using flow cytometry, as detailed in the Materials and Methods section. % Annexin V positive cells **(B)** or %Annexin V, %Annexin V +PI positive cells in **(A)** were plotted as means of triplicate determinations in a representative experiment; similar results were obtained in at least two additional experiments. **(A)** Plotted data is the mean of each treatment set. Additional details of the

Molecular Pharmacology Fast Forward. Published on December 5, 2014 as DOI: 10.1124/mol.114.093211
This article has not been copyedited and formatted. The final version may differ from this version.

data set (mean, SD, number of observations) are provided as a table in Supplemental Figure 1. P-values are reported, as shown. **(B)** Mean ± S.D. are plotted for each measurement. * indicates $p < 0.001$

Figure 5 Treatment of MDA-MB-436 cells with R9-cc-caPeptide inhibits colony formation. (A) MDA-MB-436 ($3x10^5$) cells were treated with increasing concentrations of either R9-cc-caPeptide or R9-cc-scrambled for one hour, removed from the flask, and plated at 750 cells per 10 cm dish, and incubated for 14 days. Colonies were then counted, as detailed in the Materials and Methods section. Colonies formed are the means (± S.D.) of triplicate determinations in a representative experiment; similar results were obtained in at least two additional experiments. Representative images of treated plates are provided in Supplemental Figure 2.

Figure 6 R9-cc-caPeptide treatment inhibits the association of PCNA with chromatin. MDA-MB-436 cells were treated with 30 µM of R9-cc-caPeptide for 8 hours, followed by separation of the NP-40 extractable fraction (NP-E, free form of PCNA) and NP-40 resistant fraction (NP-E, chromatin associated PCNA). Fractions were then analyzed, as detailed in the Materials and Methods section. Plotted values represent the mean (± S.D.) of the normalized density (versus the control) of a total of three different experiments.

Figure 7 R9-cc-caPeptide treatment effectively reduces tumor volume in a mouse model. A) NSG mice were randomly divided into 3 groups of 6 mice after each being injected with $5x10^6$ MDA-MB-436 cells in Matrigel. Each group was treated with PBS (circle), R9-cc-caPeptide (square), or R9-cc-scrambled (triangle) 3 times a week via intratumoral injection. Tumor sizes were measured at indicated time points and tumor volumes were estimated based on the length (L) and width (W) of the tumors ($V = L \times W^2 \times 0.5$). The mean tumor volume for each tumor group was graphed (± S.D.). * indicates $p<0.05$. **B)** Tumor masses were measured at the end of the experiment and graphed in a scatter plot with mean (± S.D.).

Figure 8 Various cancer cell types exhibit a range of sensitivity to R9-cc-caPeptide treatment. (A) Exponentially growing ($3x10^3$) MDA-MB-436, MCF 7, PaCa-2, and U937 cells were treated with increasing concentrations of R9-cc-caPeptide for 48 hours. **(B)** HCC 1937 cells (both with and without BRCA1) were treated with increasing concentrations of R9-cc-caPeptide for 48 hours. All cells were evaluated for cell survival, as compared to untreated control cells for each cell type using the MTT assay (as detailed in the Materials and Methods section). Data points are means (± S.D.) of octuplicate determinations in a representative experiment; similar results were obtained in at least three additional experiments. * indicates $p < 0.001$

Figure 9 Specific amino acids within the caPeptide sequence are critical to the observed cytotoxicity and correlate with *in silico* molecular modeling of region of interest. (A) Exponentially growing ($1x10^6$) MDA-MB-436 cells were incubated with 75 µM of R9-caPeptide or R9-cc-alanine substituted caPeptides for 24 hours. The cells were then analyzed by flow cytometry. % cell death was calculated in reference to control cells (no peptide treatment), with standard deviation displayed from an average of 5 separate experiments. Representative FACS analyses are shown in Supplemental Figure 3. **(B)** Crystal structure of FEN-1 binding to PCNA, with caPeptide amino acids highlighted (PDB ID: 1UL1, Sakurai et al., 2005).

Molecular Pharmacology Fast Forward. Published on December 5, 2014 as DOI: 10.1124/mol.114.093211
This article has not been copyedited and formatted. The final version may differ from this version.

Figure 1

A

Antibody	Amino Acids	Sequence	Dilution for Western Blot	Specificity for caPCNA
Ab122	122-133	DVEQLGIPEQEY	1:500	Not Specific
Ab124	124-133	EQLGIPEQEY	1:500	Not Specific
Ab125	125-133	QLGIPEQEY	1:500	Specific
Ab126	126-133	LGIPEQEY	1:500	Specific
Ab135	126-135	LGIPEQEYSC	1:500	Specific
Ab138	126-138	LGIPEQEYSCVVK	1:500	Not Specific
Ab143	126-143	LGIPEQEYSCVVKMPSGE	1:500	Not Specific
Ab153	126-153	LGIPEQEYSCVVKMPSGEFARICRDLSH	1:500	Not Specific
Ab163	126-163	LGIPEQEYSCVVKMPSGEFARICRDLSHIGDAVVISCA	1:500	Not Specific

B

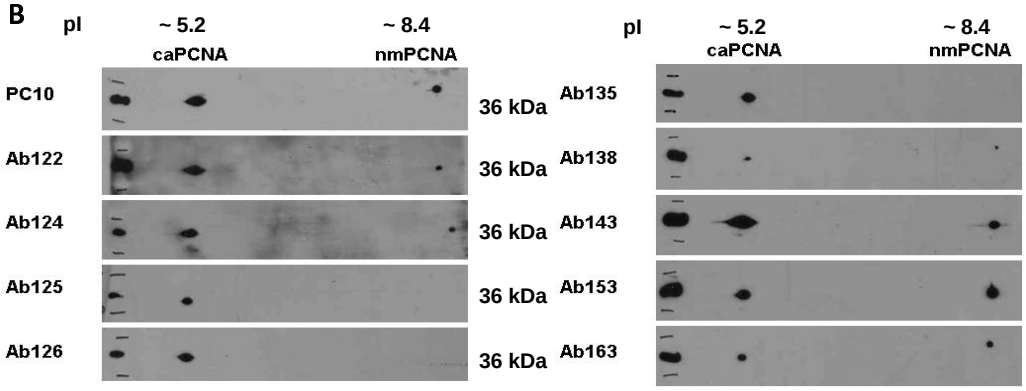

C

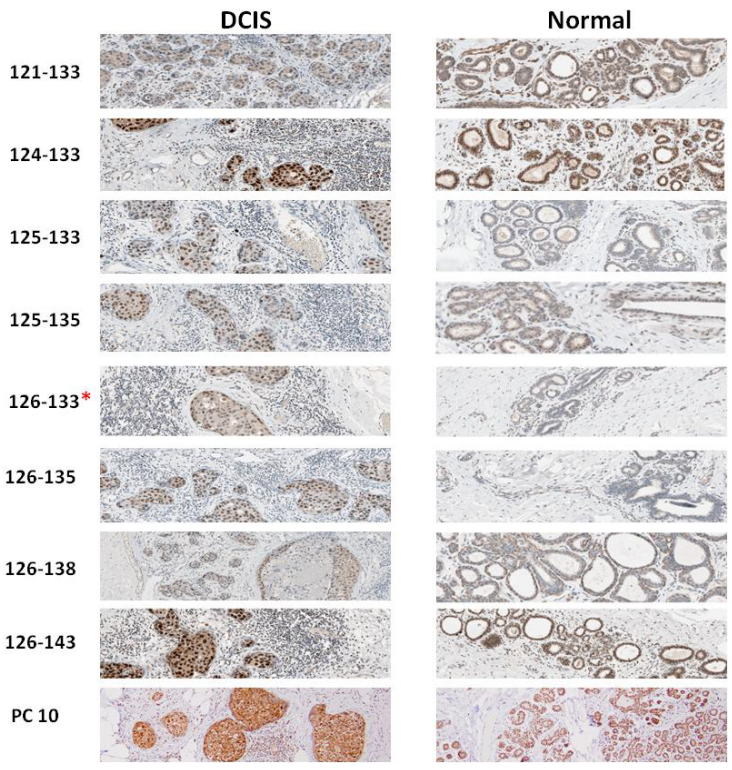

Figure 2

A

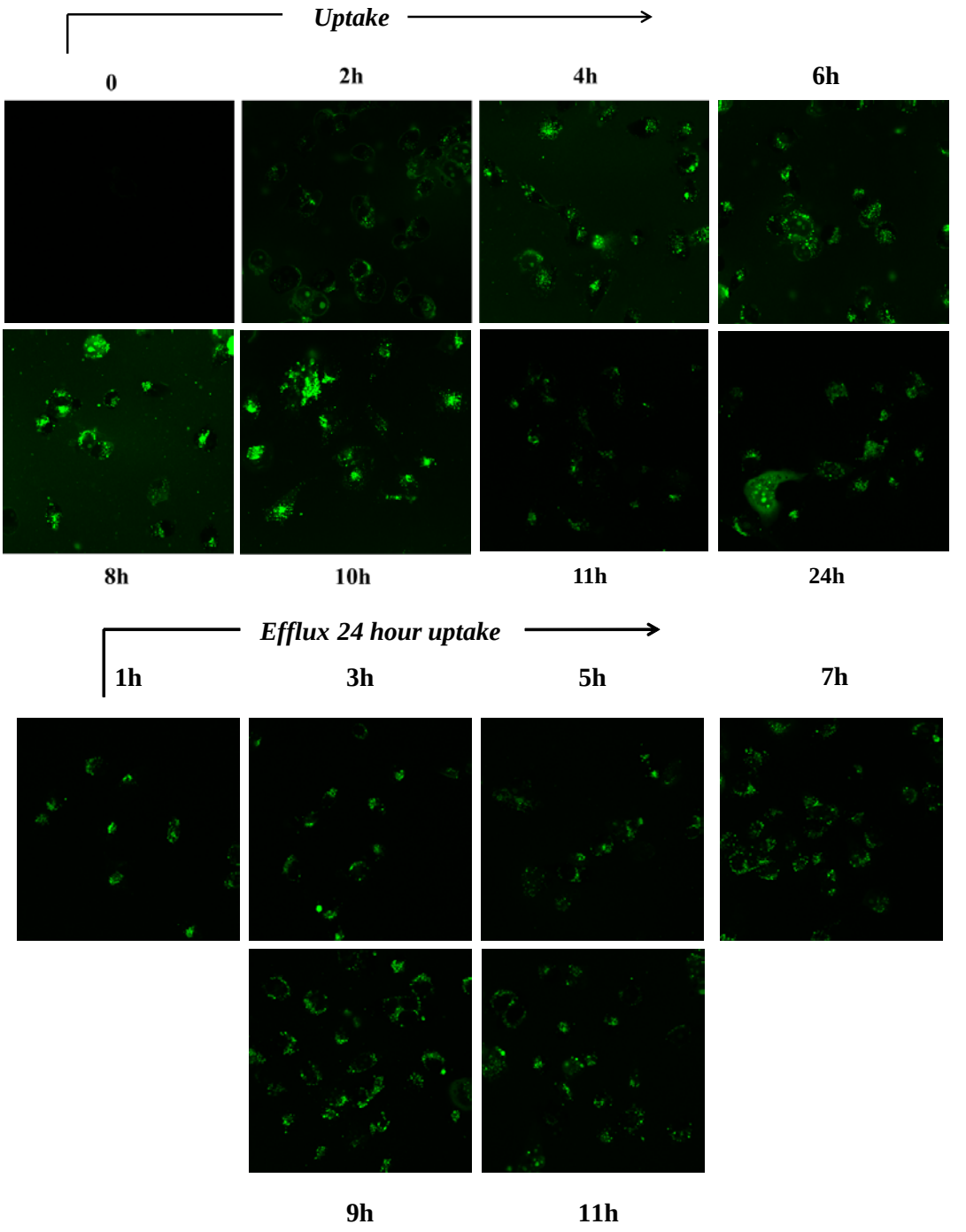
Uptake
0
2h
4h
6h
8h
10h
11h
24h
Efflux 24 hour uptake
1h
3h
5h
7h
9h
11h

B

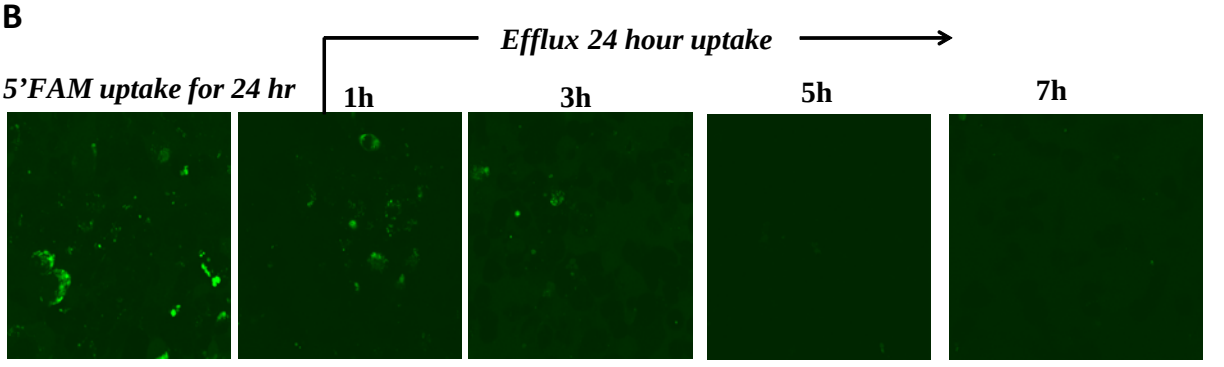
5'FAM uptake for 24 hr
Efflux 24 hour uptake
1h
3h
5h
7h

Molecular Pharmacology Fast Forward. Published on December 5, 2014 as DOI: 10.1124/mol.114.093211
This article has not been copyedited and formatted. The final version may differ from this version.

Figure 3

A

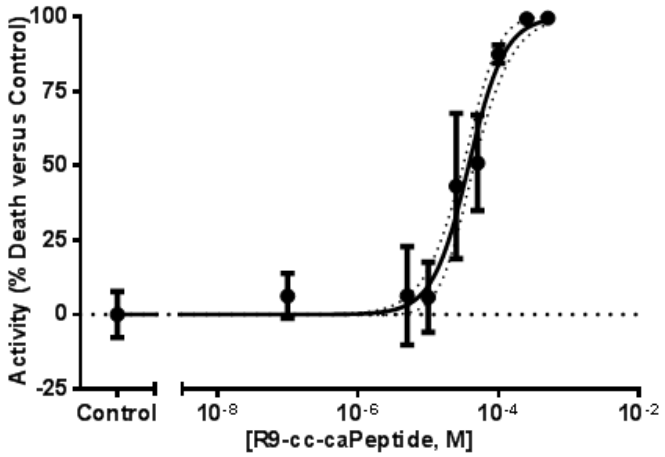

B

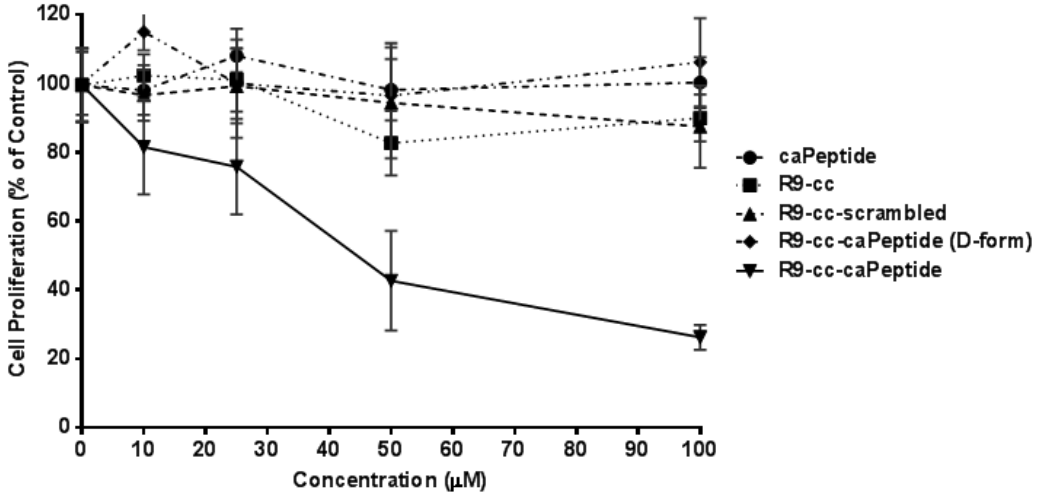

C

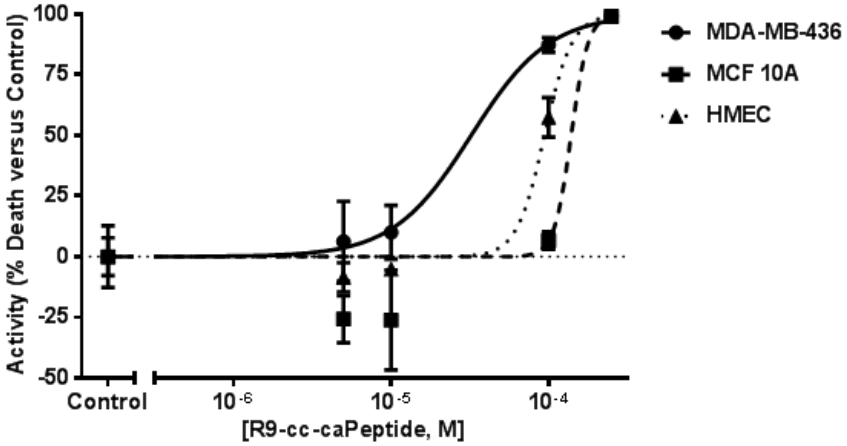

Molecular Pharmacology Fast Forward. Published on December 5, 2014 as DOI: 10.1124/mol.114.093211
This article has not been copyedited and formatted. The final version may differ from this version.

Figure 4

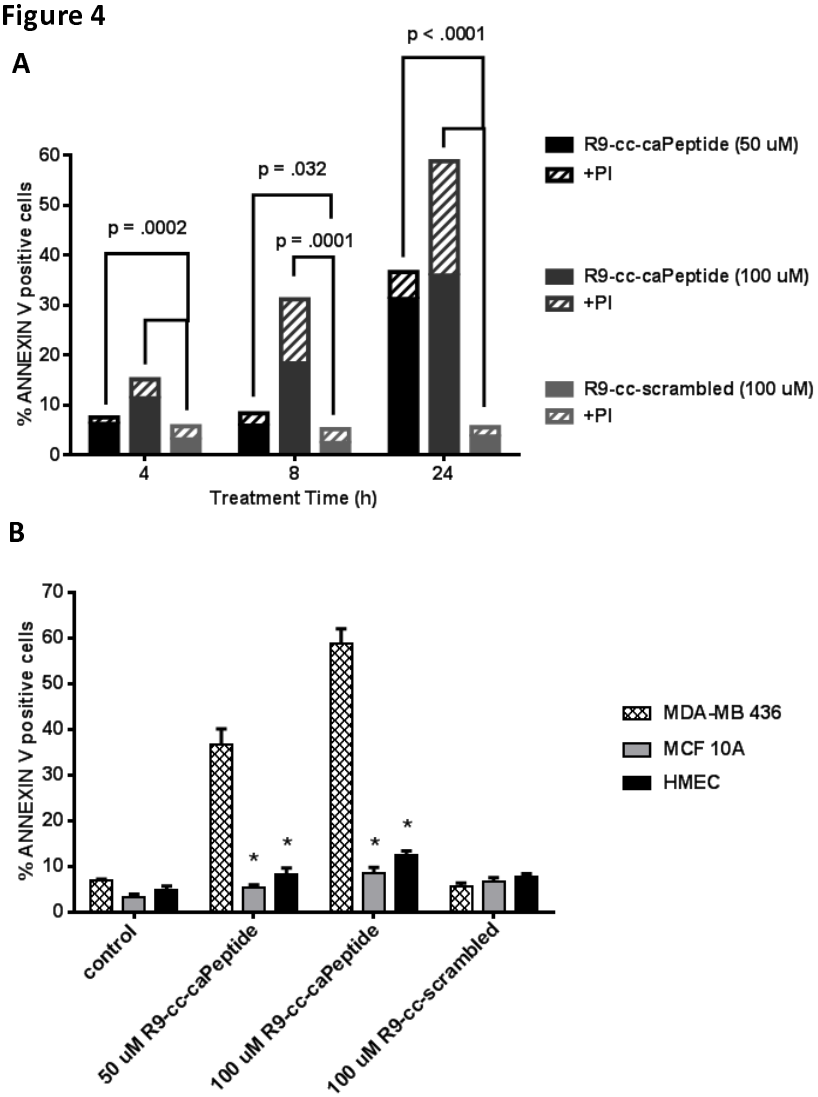

Figure 5

A

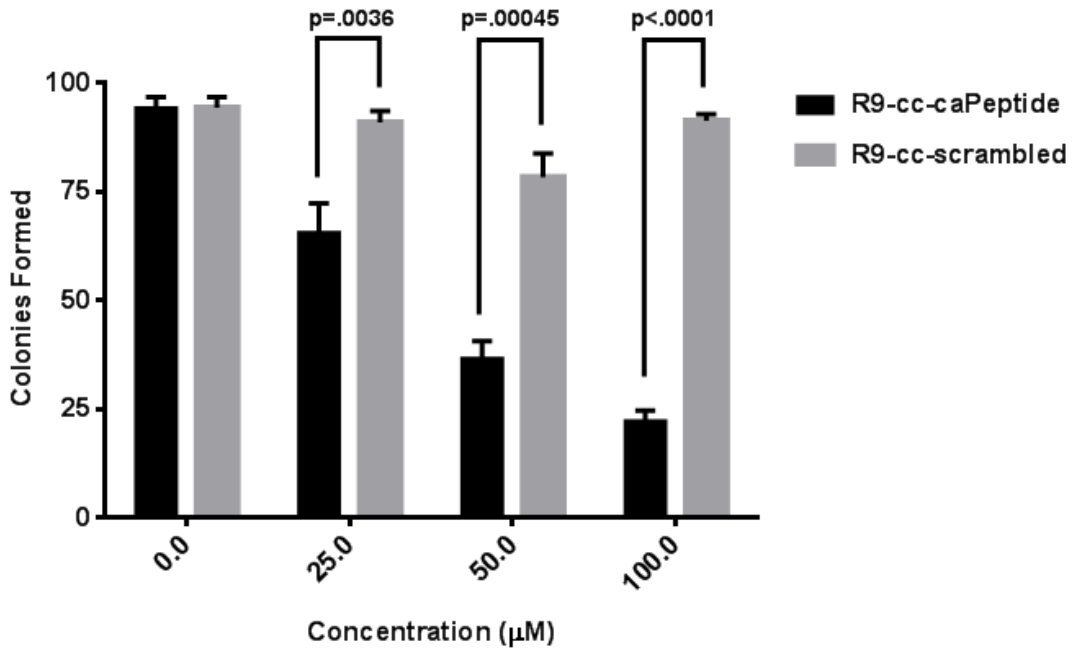

Figure 6

Figure 7

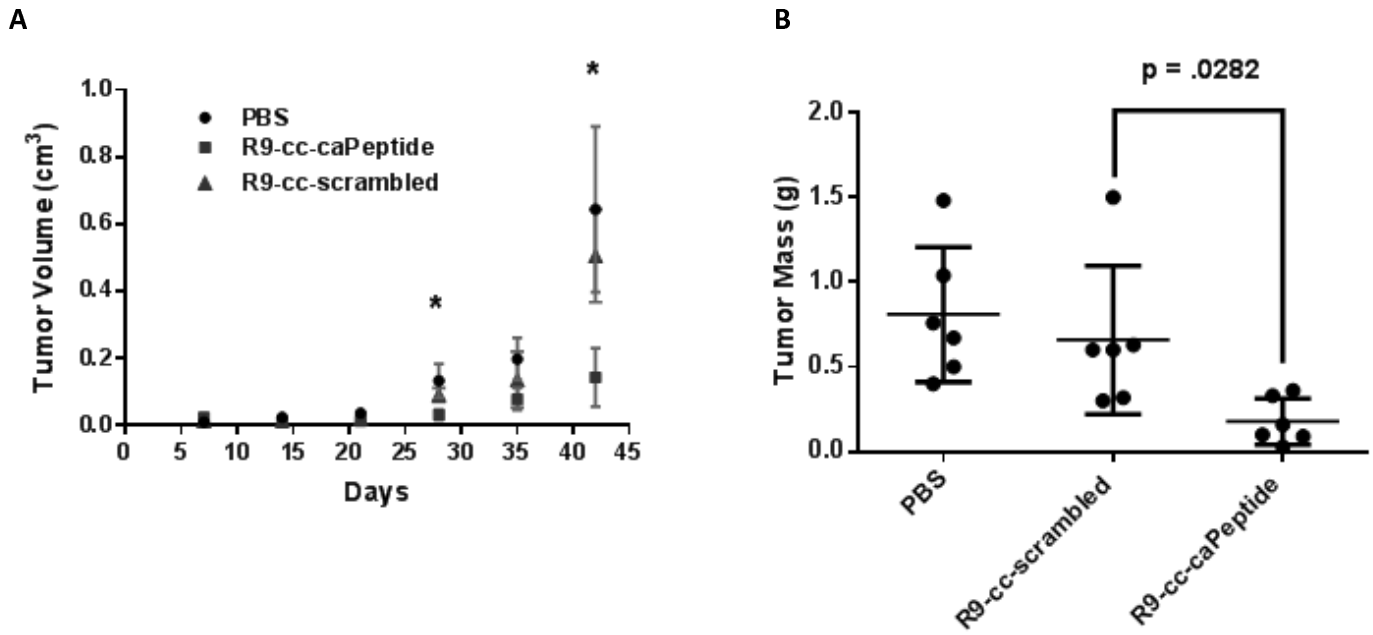

Molecular Pharmacology Fast Forward. Published on December 5, 2014 as DOI: 10.1124/mol.114.093211
This article has not been copyedited and formatted. The final version may differ from this version.

Figure 8

A

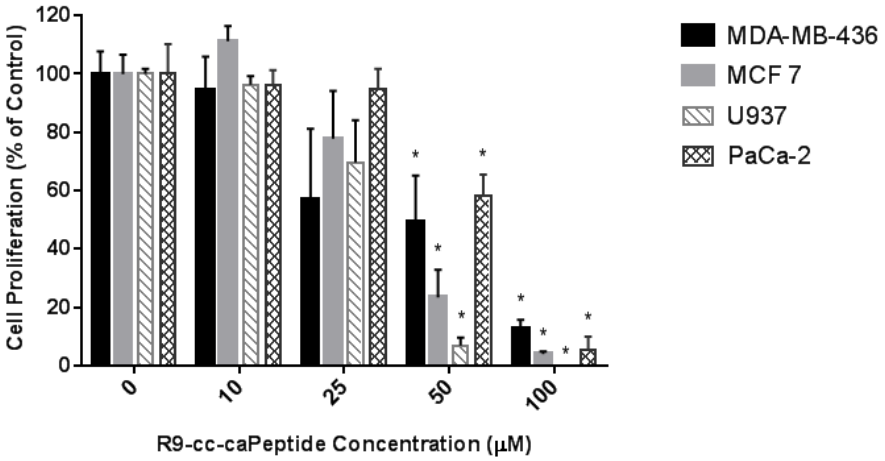

B

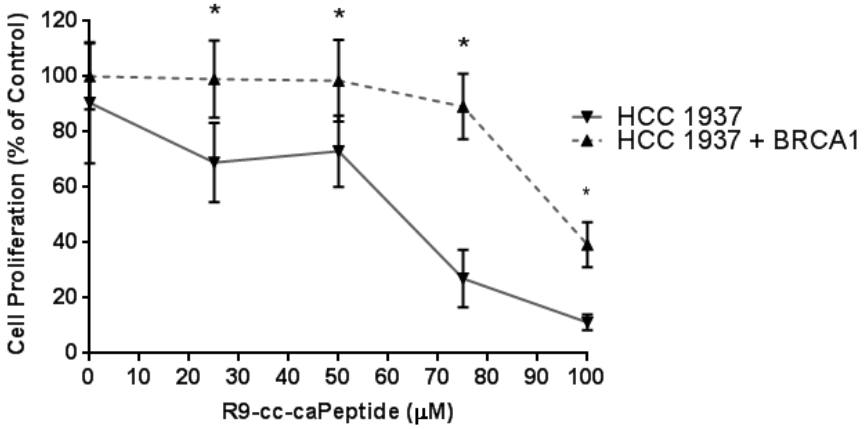

Molecular Pharmacology Fast Forward. Published on December 5, 2014 as DOI: 10.1124/mol.114.093211
This article has not been copyedited and formatted. The final version may differ from this version.

Figure 9

A

Peptide	% Death ± SD
R9-caPeptide	45.7 ± 1.8
scrambled	4.8 ± 0.8
R9-L126A	7.6 ± 0.9
R9-G127A	58.4 ± 2.8
R9-I128A	10.5 ± 1.3
R9-P129A	52.8 ± 1.0
R9-E130A	10.3 ± 0.5
R9-Q131A	82.8 ± 1.0
R9-E132A	13.8 ± 0.5
R9-Y133A	.1 ± 1.1

B

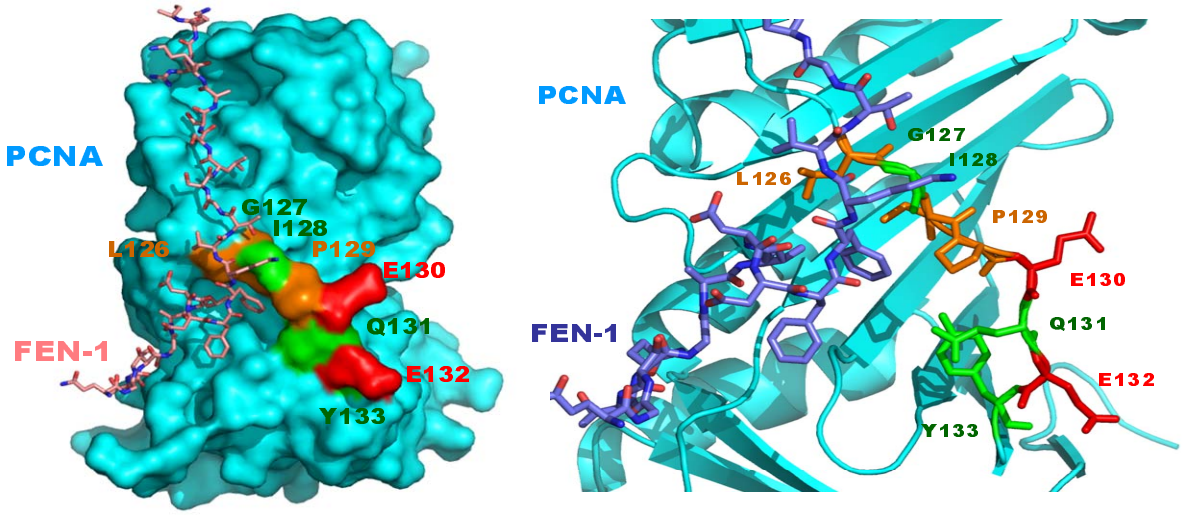

A Peptide Mimicking a Region in Proliferating Cell Nuclear Antigen (PCNA) Specific to Key Protein Interactions is Cytotoxic to Breast Cancer

Shanna J. Smith, Long Gu, Elizabeth A. Phipps, Lacey E. Dobrolecki, Karla S. Mabrey, Pattie Gulley, Kelsey L. Dillehay, Zhongyun Dong, Gregg B. Fields, Yun-Ru Chen, David Ann, Robert J. Hickey, and Linda H. Malkas

Molecular Pharmacology

Supplemental Information

Figure S1

	50 uM R9-caPep						100 uM R9-caPep						100 uM R9-scrambled					
	Annexin			PI			Annexin			PI			Annexin			PI		
	4 h	8 h	24 h	4 h	8 h	24 h	4 h	8 h	24 h	4 h	8 h	24 h	4 h	8 h	24 h	4 h	8 h	24 h
Average (%)	6.2667	5.8667	31.2667	1.2667	2.5000	5.3667	11.3667	18.3667	35.9667	3.8000	12.8333	22.8333	3.1000	2.4333	3.7000	2.6667	2.7667	1.8667
Std Dev (%)	0.4041	1.8175	2.2502	0.2082	0.3000	1.3013	1.0970	1.7616	2.4420	0.3606	2.6026	1.1719	0.1732	0.3215	0.6557	0.8963	0.3512	0.2517
# Observations	3	3	3	3	3	3	3	3	3	3	3	3	3	3	3	3	3	3

Summary of flow cytometry data from Figure 4A. Exponentially growing ($1x10^6$) MDA-MB-436 cells were treated with increasing concentrations of R9-cc-caPeptide or 100 μM R9-cc-scrambled up to 24 hours. Annexin V staining was then evaluated using flow cytometry, as detailed in the Materials and Methods section. The mean and standard deviation (Std Dev) of the %Annexin V and %Annexin V +PI positive cells, and number of observations for each time point are provided to supplement Figure 4A.

A Peptide Mimicking a Region in Proliferating Cell Nuclear Antigen (PCNA) Specific to Key Protein Interactions is Cytotoxic to Breast Cancer

Shanna J. Smith, Long Gu, Elizabeth A. Phipps, Lacey E. Dobrolecki, Karla S. Mabrey, Pattie Gulley, Kelsey L. Dillehay, Zhongyun Dong, Gregg B. Fields, Yun-Ru Chen, David Ann, Robert J. Hickey, and Linda H. Malkas

Molecular Pharmacology

Supplemental Information

Figure S2

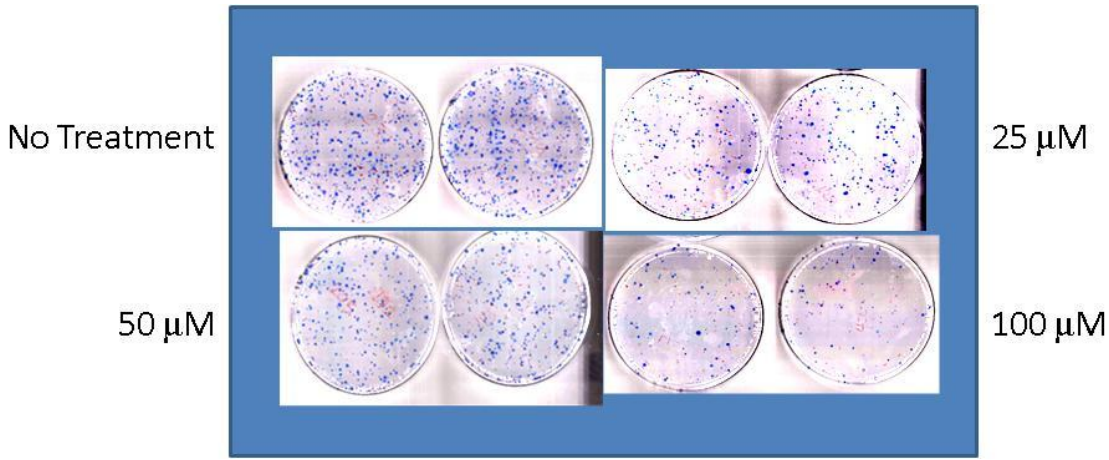

Representative images of colony formation assay. MDA-MB-436 ($3x10^5$) cells were treated with increasing concentrations of R9-cc-caPeptide for one hour, removed from the flask, and plated at 750 cells per 10 cm dish, and incubated for 14 days. Colonies were then counted, as detailed in the Materials and Methods section. Representative plates for each R9-cc-caPeptide treatment are shown.

A Peptide Mimicking a Region in Proliferating Cell Nuclear Antigen (PCNA) Specific to Key Protein Interactions is Cytotoxic to Breast Cancer

Shanna J. Smith, Long Gu, Elizabeth A. Phipps, Lacey E. Dobrolecki, Karla S. Mabrey, Pattie Gulley, Kelsey L. Dillehay, Zhongyun Dong, Gregg B. Fields, Yun-Ru Chen, David Ann, Robert J. Hickey, and Linda H. Malkas

Molecular Pharmacology

Supplemental Information

Figure S3

control – no treatment

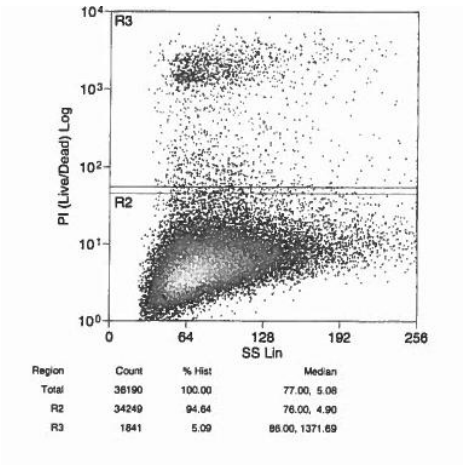

75 μM R9-cc-caPeptide

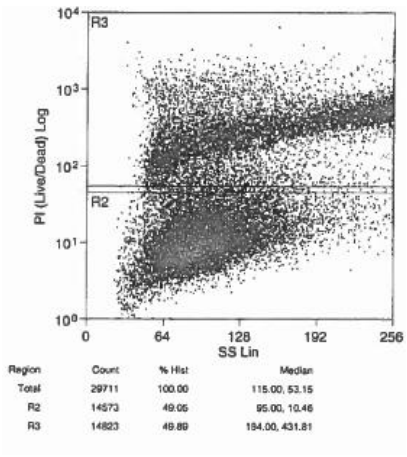

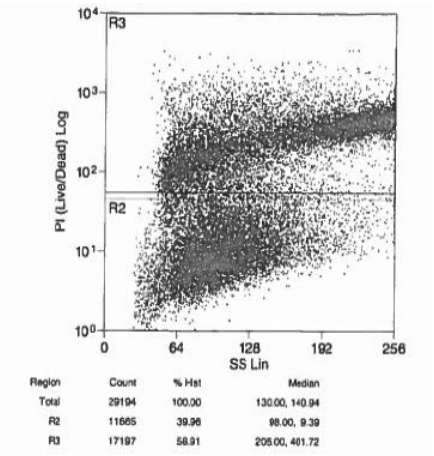

similar response

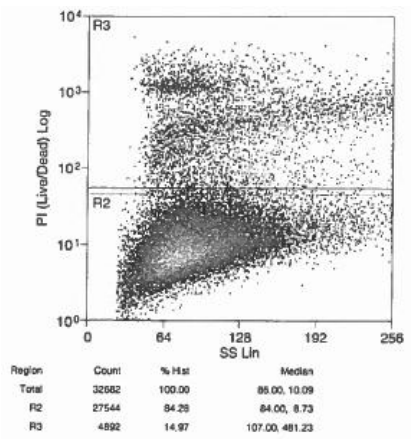

decreased cytotoxicity

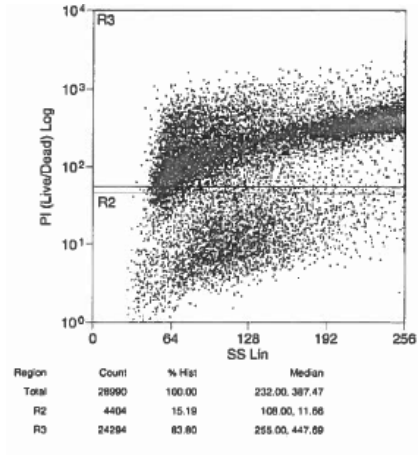

increased cytotoxicity

Representative flow cytometry data for alanine scanning experiment. Exponentially growing ($1x10^6$) MDA-MB-436 cells were incubated with 75 μM of R9-caPeptide or R9-cc-alanine substituted caPeptides for 24 hours. The cells were then analyzed by flow cytometry. % cell death was calculated in reference to control cells (no peptide treatment), with standard deviation displayed from an average of 5 separate experiments. A decrease of cell death indicates the amino acid substituted is critical to the cytotoxicity of the peptide sequence.